A CLASS OF SHORT-TERM RECURRENCE ANDERSON MIXING METHODS AND THEIR APPLICATIONS

Anonymous authors
Paper under double-blind review

ABSTRACT

Anderson mixing (AM) is a powerful acceleration method for fixed-point iterations, but its computation requires storing many historical iterations. The extra memory footprint can be prohibitive when solving high-dimensional problems in a resource-limited machine. To reduce the memory overhead, we propose a novel class of short-term recurrence AM methods (ST-AM). The ST-AM methods only store two previous iterations with cheap corrections. We prove that the basic version of ST-AM is equivalent to the full-memory AM in strongly convex quadratic optimization, and with minor changes it has local linear convergence for solving general nonlinear fixed-point problems. These properties guarantee the theoretical advantages of ST-AM over classical gradient-based methods. We further propose the regularized ST-AM and analyze its convergence properties for nonconvex (stochastic) optimization. Finally, we apply ST-AM to several applications including training neural networks in image classification and language tasks. Experimental results show that ST-AM is competitive with the long-memory AM and outperforms many existing optimizers, including SGD and ADAM.

1 INTRODUCTION

Anderson mixing (AM) (Anderson, 1965) is a sequence acceleration method (Brezinski et al., 2018) in scientific computing. It is widely used to accelerate the slow convergence of nonlinear fixed-point iterations (Lin et al., 2019; Fu et al., 2020; An et al., 2017) , e.g. the self-consistent field iterations in electronic structure computations (Garza & Scuseria, 2012; Arora et al., 2017). Specifically, we consider a fixed-point iteration $x_{k+1} = g(x_k), k = 0, 1, \ldots,$ where $g : \mathbb{R}^d \to \mathbb{R}^d$ is the fixed-point map. By using m historical iterations, AM(m) aims to extrapolate a new iterate that satisfies certain optimality property. When the function evaluation is costly, the reduction of the number of iterations brought by AM can save large amount of computation (Fang & Saad, 2009).

AM can be used as a method for solving nonlinear equations (Kelley, 2018) as the fixed-point $x = g(x)$ is equivalent to $h(x) := x - g(x) = 0$. In practice, since computing the Jacobian of $h(x)$ is commonly difficult or even unavailable (Nocedal & Wright, 2006), AM can be seen as a practical alternate for Newton's method (An et al., 2017). Also, compared with the classical iterative methods such as the nonlinear conjugate gradient (CG) method (Hager & Zhang, 2006), no line-search or trust-region technique is used in AM, which is preferable for large-scale unconstrained optimization. Empirically, it is observable that AM can largely accelerate convergence, though its theoretical analysis is still under-explored. It turns out that in the linear case (Walker & Ni, 2011; Potra & Engler, 2013), the full-memory AM ($m = k$) is essentially equivalent to GMRES (Saad & Schultz, 1986), a powerful Krylov subspace method that can exhibit superlinear convergence behaviour in solving linear systems (Van der Vorst & Vuik, 1993). For general nonlinear problems, AM is recognized as a multisecant quasi-Newton method (Fang & Saad, 2009; Brezinski et al., 2018). As far as we know, only local linear convergence has been obtained for the limited-memory AM ($m < k$) in general (Toth & Kelley, 2015; Evans et al., 2020; De Sterck & He, 2021).

For the application of AM, one of the major concerns is the historical length m, a critical factor related to the efficiency of AM (Walker & Ni, 2011). A larger m can incorporate more historical information into one extrapolation. However, it incurs heavier memory overhead since $2m$ vectors of dimension d need to be stored in AM(m). The additional memory footprint can be prohibitive for solving high-dimensional problems in a resource-limited machine (Deng, 2019). Using small

m can alleviate the memory overhead but may deteriorate the efficacy of AM since much historical information is omitted in the extrapolation (Walker & Ni, 2011; Evans et al., 2020).

To address the memory issue of AM, we deeply investigate the properties of the historical iterations produced by AM and leverage them to develop the short-term recurrence variant, namely ST-AM. The basic version of ST-AM imposes some *orthogonalization* property on the historical sequence, which is inspired by the CG method (Hestenes & Stiefel, 1952) that enjoys a three-term recurrence for solving symmetric positive definite (SPD) linear systems. Furthermore, to better suit the more difficult nonconvex optimization, a regularized short-term form is introduced. We highlight the main contributions of our work as follows.

1. We develop a novel class of short-term recurrence AM methods (ST-AM), including the basic ST-AM, the modified ST-AM (MST-AM), and the regularized ST-AM (RST-AM). The basic ST-AM is applicable for solving linear systems, the MST-AM can solve general fixed-point problems, and RST-AM aims for solving stochastic optimization. An important feature of ST-AM is that all methods only need to store two previous iterations with cheap corrections, which significantly reduces the additional memory requirement compared with the classical AM.
2. A complete theoretical analysis of the ST-AM methods is given. When solving strongly convex quadratic optimization, we prove that the basic ST-AM is equivalent to full-memory AM and has the same convergence rate as CG method. Moreover, it is proved that MST-AM has local linear convergence for solving fixed-point problems. These theoretical properties guarantee the advantages of ST-AM over the first-order methods. Besides, we establish the global convergence property and complexity analysis for RST-AM when solving stochastic optimization problems.
3. The experiments on solving linear systems and cubic-regularized quadratic problems are consistent with the theoretical results for the basic ST-AM and MST-AM. Furthermore, extensive experiments on training deep neural networks for image classification and language modeling show that RST-AM is competitive with the long-memory AM and outperforms many existing optimizers such as SGD and ADAM.

2 Related work

AM is also known as an *extrapolation algorithm* in scientific computing (Anderson, 2019). A parallel method is Shanks transformation (Shanks, 1955) which also uses long historical sequences to improve slowly convergent or divergent sequences. Related classical algorithms includes Minimal Polynomial Extrapolation (Cabay & Jackson, 1976) and Reduced Rank Extrapolation (Eddy, 1979), and a framework of these extrapolation algorithms including AM is given in (Brezinski et al., 2018). Note that an elegant recursive algorithm named ϵ-algorithm has been discovered for Shanks transformation for scalar sequence (Wynn, 1956), and was later generalized as the vector ϵ-algorithm (Wynn, 1962) for handling vector sequences, but this short-term recurrence form is not equivalent to the original Shanks transformation in general (Brezinski & Redivo-Zaglia, 2017). Since AM is closely related to quasi-Newton methods (Fang & Saad, 2009), there are also some works trying to derive equivalent forms of the full-memory quasi-Newton methods using limited memory (Kolda et al., 1998; Berahas et al., 2021), while no short-term recurrence is available. To the best of our knowledge, ST-AM is the first attempt to short-term recurrence quasi-Newton methods.

Recently, there have been growing demands for solving large-scale and high-dimensional fixed-point problems in scientific computing (Lin et al., 2019) and machine learning (Bottou et al., 2018). For these applications, Newton-like methods (Byrd et al., 2016; Wang et al., 2017; Mokhtari et al., 2018) are less appealing due to the heavy memory and computational cost, especially in nonconvex stochastic optimization, where only sublinear convergence can be expected if only stochastic gradients can be accessed (Nemirovskij & Yudin, 1983). On the other side, first-order methods (Necoara et al., 2019) stand out for their low per-iteration cost, though the convergence can be slow in practice. When training neural networks, SGD with momentum (SGDM) (Qian, 1999), and adaptive learning rate methods, e.g. AdaGrad (Duchi et al., 2011), RMSprop (Tieleman & Hinton, 2012), Adam, are very popular optimizers. Our proposed ST-AM methods have the nature of quasi-Newton methods while the memory footprint is largely reduced to be close to first-order methods. Thus, ST-AM can be a competitive optimizer from both theoretical and practical perspectives.

3 METHODOLOGY

In this section, we give the details of the proposed ST-AM. In the following context, we always assume the objective function as $f : \mathbb{R}^d \to \mathbb{R}$, the fixed-point map $g : \mathbb{R}^d \mapsto \mathbb{R}^d$. Moreover, we do not distinguish $r_k = -\nabla f(x_k)$ and $r_k = g(x_k) - x_k$ in our discussion as $\nabla f(x) = 0$ is equivalent to $g(x) = -\nabla f(x) + x = x$.

3.1 ANDERSON MIXING

The AM finds the fix-point of g via maintaining two sequences of length $m(m \leq k)$:

$$X_k = [\Delta x_{k-m}, \Delta x_{k-m+1}, \cdots, \Delta x_{k-1}], R_k = [\Delta r_{k-m}, \Delta r_{k-m+1}, \cdots, \Delta r_{k-1}], \tag{1}$$

where the operator Δ denotes the forward difference, e.g. $\Delta x_k = x_{k+1} - x_k$. Each update of AM can be decoupled into two steps, namely *the projection step* and *the mixing step*:

$$\bar{x}_k = x_k - X_k \Gamma_k, \quad \text{(Projection step)}, \quad x_{k+1} = \bar{x}_k + \beta_k \bar{r}_k, \quad \text{(Mixing step)}, \tag{2}$$

where $\bar{r}_k := r_k - R_k \Gamma_k$ and $\beta_k > 0$ is the mixing parameter. The coefficients Γ_k is determined by

$$\Gamma_k = \arg\min_{\Gamma \in \mathbb{R}^m} \|r_k - R_k \Gamma\|_2. \tag{3}$$

Thus, the full form of AM (Fang & Saad, 2009; Walker & Ni, 2011) is

$$x_{k+1} = x_k + \beta_k r_k - (X_k + \beta_k R_k)\, \Gamma_k. \tag{4}$$

Remark 1. *To see the rationality of AM, assume g is continuously differentiable, then we have $h(x_j) - h(x_{j-1}) \approx h'(x_k)(x_j - x_{j-1})$ around x_k, where $h'(x_k)$ is the Jacobian of $h(x) := x - g(x)$. So, it is reasonable to assume $R_k \approx -h'(x_k) X_k$, and we see $\|r_k - R_k \Gamma\|_2 \approx \|r_k + h'(x_k) X_k \Gamma\|_2$. Thus, we can recognize (3) as solving $h'(x_k) d_k = h(x_k)$ in a least-squares sense, where $d_k = X_k \Gamma_k$. The mixing step incorporates r_k to the new update x_{k+1} if $\beta_k > 0$. Otherwise, $x_{k+1} = \bar{x}_k$ is an interpolation of the previous iterates, leading to a stagnating sequence.*

3.2 THE BASIC SHORT-TERM RECURRENCE ANDERSON MIXING

The basic ST-AM is to solve the strongly convex quadratic optimization:

$$\min_{x \in \mathbb{R}^d} f(x) := \frac{1}{2} x^{\mathrm{T}} A x - b^{\mathrm{T}} x, \tag{5}$$

where $A \succ 0$. At the k-th iteration, given the two matrices $P_{k-1} = (p_{k-2}, p_{k-1}) \in \mathbb{R}^{d \times 2}, Q_{k-1} = (q_{k-2}, q_{k-1}) \in \mathbb{R}^{d \times 2}$ and defining $p = x_k - x_{k-1}$ and $q = r_k - r_{k-1}$, the basic ST-AM constructs

$$\tilde{p} = p - P_{k-1}(Q_{k-1}^{\mathrm{T}} q), \quad \tilde{q} = q - Q_{k-1}(Q_{k-1}^{\mathrm{T}} q), \tag{6a}$$

$$p_k = \tilde{p}/\|\tilde{q}\|_2, \quad q_k = \tilde{q}/\|\tilde{q}\|_2. \tag{6b}$$

Then, we update $P_k = (p_{k-1}, p_k), Q_k = (q_{k-1}, q_k) \in \mathbb{R}^{d \times 2}$. It is easy to know $Q_k^{\top} Q_k = I_2$ and the storage of P_k and Q_k is equal to AM(2). With the corrected P_k and Q_k, the ST-AM method modifies the projection and mixing step accordingly, that is,

$$\bar{x}_k = x_k - P_k \Gamma_k, \quad \text{(Projection step)}, \quad x_{k+1} = \bar{x}_k + \beta_k \bar{r}_k, \quad \text{(Mixing step)}, \tag{7}$$

where $\Gamma_k = \arg\min \|r_k - Q_k \Gamma\|_2 = Q_k^{\mathrm{T}} r_k$ and $\bar{r}_k = r_k - Q_k \Gamma_k$. Thus, the ST-AM replaces X_k and R_k in (1) by P_k and Q_k respectively and imposes the orthogonalization property for Q_k. The details of basic ST-AM are given in Algorithm 2 in Appendix A.1. Define $\bar{P}_k = (p_1, p_2, \ldots, p_k), \bar{Q}_k = (q_1, q_2, \ldots, q_k)$, the Krylov subspace $\mathcal{K}_m(A, v) \equiv span\{v, Av, A^2 v, \ldots, A^{m-1} v\}$, the range of X as $range(X)$, we give the properties for the basic ST-AM in Theorem 1.

Theorem 1. *Let $\{x_k\}$ be the sequence generated by the basic ST-AM, the following properties hold:*
(i) $\|\tilde{q}\|_2 > 0, range(\bar{P}_k) = range(X_k) = \mathcal{K}_k(A, r_0), range(\bar{Q}_k) = range(R_k) = A\mathcal{K}_k(A, r_0)$;
(ii) $\bar{Q}_k = -A\bar{P}_k, \bar{Q}_k^{\mathrm{T}} \bar{Q}_k = I_k$;
(iii) $\bar{r}_k \perp range(\bar{Q}_k)$ and $\bar{x}_k = x_0 + z_k$, where $z_k = \arg\min_{z \in \mathcal{K}_k(A, r_0)} \|r_0 - Az\|_2$.
If $\|\bar{r}_k\|_2 = 0$, then x_{k+1} is the exact solution.

The proof is in Appendix A.1. It is noted that the property (iii) in Theorem 1 exactly describes the relation $\bar{x}_k = x_k^{\mathrm{G}}$, where x_k^{G} is output of the k-th iteration of GMRES (Saad, 2003). Moreover, let $\bar{x}_k^{\mathrm{F}}$ be the k-th intermediate iterate in full-memory AM($m = k$), we prove that $\bar{x}_k^{\mathrm{F}} = x_k^{\mathrm{G}}$ (See Proposition 1 in Appendix A.1.), which induces that $\bar{x}_k = \bar{x}_k^{\mathrm{F}} = \bar{x}_k^{\mathrm{G}}$. This equivalence shows that the ST-AM mimics the long-memory AM by storing only two historical iterations. Moreover, by directly applying the convergence analysis of GMRES (Corollary 6.33 in (Saad, 2003)), we obtain the convergence rate of the basic ST-AM for solving (5):

Corollary 1. *Suppose the eigenvalues of A lies in $[\mu, L]$ with $\mu > 0$, and let $\{x_k\}$ be the sequence generated by the basic ST-AM, then the k-th intermediate residual $\bar{r}_k$ satisfies $\|\bar{r}_k\|_2 \leq \left(\frac{\sqrt{L/\mu}-1}{\sqrt{L/\mu}+1}\right)^k \|r_0\|_2$. Moreover, the algorithm finds the exact solution in at most d iterations.*

Remark 2. *The GMRES can be simplified to an elegant three-term recurrence algorithm called the* conjugate residual *(CR) method (Algorithm 6.20 in (Saad, 2003)) when solving (5). Thus, it is natural to expect a similar short-term recurrence algorithm can be conceived by carefully modifying X_k, R_k to satisfy some orthogonalization property. Since the mixing step disrupts the minimal residual property obtain in (3), one more historical iteration has to be incorporated to counteract it.*

3.3 THE MODIFIED SHORT-TERM RECURRENCE ANDERSON MIXING

For general nonlinear fixed-point iteration, global convergence may be unavailable for the basic ST-AM, as a counter-example exists for full-memory AM (Mai & Johansson, 2020). Thus, we propose a modified version of the basic ST-AM (MST-AM) and prove the local linear convergence rate under similar conditions used in (Toth & Kelley, 2015; Evans et al., 2020). Concretely, the MST-AM has three main changes with the basic ST-AM and we list them as follows.

Change 1: Instead of using the normalization step (6b), the MST-AM constructs p_k and q_k via:

$$\zeta_k = (Q_{k-1}^{\mathrm{T}} Q_{k-1})^{\dagger} Q_{k-1}^{\mathrm{T}} q, \quad p_k = p - P_{k-1}\zeta_k, \quad q_k = q - Q_{k-1}\zeta_k, \tag{8}$$

where " $\dagger$ " is the Moore-Penrose inverse. Accordingly, we choose $\Gamma_k = \arg\min \|r_k - Q_k\Gamma\|_2 = (Q_k^{\mathrm{T}} Q_k)^{\dagger} Q_k^{\mathrm{T}} r_k$. This change relaxes the orthonormality for Q_k, but keeps the orthogonal condition: $Q_{k-1}^{\mathrm{T}} q_k = 0$ (in fact, $\bar{Q}_{k-1}^{\mathrm{T}} q_k = 0$). In this case, we have $\bar{Q}_k^{\mathrm{T}} \bar{Q}_k = diag\{\|q_1\|_2^2, \ldots, \|q_k\|_2^2\}$.

Change 2: MST-AM imposes the boundedness constraint of $P_{k-1}\zeta_k$ and $Q_{k-1}\zeta_k$: If $\|P_{k-1}\zeta_k\|_2 \geq c_p\|p\|_2$ or $\|Q_{k-1}\zeta_k\|_2 \geq c_q\|q\|_2$, then $P_k = P_{k-1}, Q_k = Q_{k-1}$, where $c_p > 0, c_q \in (0, 1]$ are predefined constants. It is worth mentioning that the boundedness condition is common in the analysis of AM (Toth & Kelley, 2015; Evans et al., 2020).

Change 3: MST-AM restarts, i.e. set $P_k = Q_k = \mathbf{0}$ every m iterations. This restart operation is to limit the number of higher-order terms appeared in the residual expansion in our analysis and we can set m to be a large number in practice.

The detailed description of MST-AM is given in Appendix A.2. In the next theorem, we establish the convergence rate analysis for the MST-AM.

Theorem 2. *Let $\{x_k\}$ be the sequence generated by MST-AM, $x^* \in \mathbb{R}^d$ be a fixed-point of g and m be the restarting period for MST-AM. Suppose that in the ball $\mathcal{B}(\rho) := \{x \in \mathbb{R}^d | \|x - x^*\|_2 < \rho\}$ for some $\rho > 0$, g is Lipschitz continuously differentiable and there are constant $\kappa \in (0, 1)$ and $\hat{\kappa} > 0$ with (i) $\|g(y) - g(x)\|_2 \leq \kappa\|y - x\|_2$ for every $x, y \in \mathcal{B}(\rho)$, and (ii) $\|g'(y) - g'(x)\|_2 \leq \hat{\kappa}\|y - x\|_2$ for every $x, y \in \mathcal{B}(\rho)$, where $g'(x)$ is the Jacobian of g. Then, for the k-th residual $r_k = g(x_k) - x_k$, the following bound holds:*

$$\|r_{k+1}\|_2 \leq \theta_k(|1 - \beta_k| + \kappa\beta_k)\|r_k\|_2 + \hat{\kappa}\sum_{j=0}^{m_k} \mathcal{O}\left(\|r_{k-j}\|_2^2\right). \tag{9}$$

where $\theta_k = \|\bar{r}_k\|_2/\|r_k\|_2 \leq 1$ and $k = m_k \mod m$. Moreover, if $\|x_0 - x^*\|_2$ is sufficiently small, the residuals $\{r_k\}$ converge Q-linearly, thus the errors $\{\|x_k - x^*\|_2\}$ converge R-linearly.

In a sufficiently small local region around x^*, the convergence rate is determined by the first-order term $\theta_k(|1 - \beta_k| + \kappa\beta_k)\|r_k\|_2$. Since $\bar{r}_k$ is the orthogonal projection of r_k onto the subspace $range(Q_k)^{\perp}$, θ_k has the interpretation of the direction-sine between r_k and the subspace

Algorithm 1 RST-AM for stochastic programming

Input: $x_0 \in \mathbb{R}^d, \beta_k > 0, \alpha_k \in [0,1], \delta_k^{(1)} > 0, \delta_k^{(2)} > 0$.
Output: $x \in \mathbb{R}^d$

1: $P_0, Q_0 = \mathbf{0} \in \mathbb{R}^{d\times 2}, p_0, q_0 = \mathbf{0} \in \mathbb{R}^d$
2: **for** $k = 0, 1, \ldots,$ until convergence, **do**
3: $\quad r_k = -\nabla f_{S_k}(x_k)$
4: $\quad$ **if** $k > 0$ **then**
5: $\quad\quad p = x_k - x_{k-1}, q = r_k - r_{k-1}$
6: $\quad\quad \zeta_k = (Q_{k-1}^{\mathrm{T}} Q_{k-1} + \delta_k^{(1)} P_{k-1}^{\mathrm{T}} P_{k-1})^{\dagger} Q_{k-1}^{\mathrm{T}} q$
7: $\quad\quad q_k = q - Q_{k-1}\zeta_k, p_k = p - P_{k-1}\zeta_k$
8: $\quad\quad P_k = [p_{k-1}, p_k], Q_k = [q_{k-1}, q_k]$
9: $\quad$ **end if**
10: $\quad$ Check Condition (13) and use smaller α_k if (13) is violated
11: $\quad \Gamma_k = (Q_k^{\mathrm{T}} Q_k + \delta_k^{(2)} P_k^{\mathrm{T}} P_k)^{\dagger} Q_k^{\mathrm{T}} r_k$
12: $\quad \bar{x}_k = x_k - \alpha_k P_k \Gamma_k, \bar{r}_k = r_k - \alpha_k Q_k \Gamma_k$
13: $\quad x_{k+1} = \bar{x}_k + \beta_k \bar{r}_k$
14: $\quad$ Apply learning rate schedule of α_k, β_k.
15: **end for**
16: **return** x_k

$range(Q_k)$. When θ_k is small, e.g. r_k nearly lies in $range(Q_k)$, the acceleration by MST-AM is significant. For the special case of solving SPD linear systems, the global orthogonalization property holds, i.e. $\bar{r}_k \perp range(\bar{Q}_k)$, so the acceleration can be even more significant. Our experimental results also validate the acceleration of the MST-AM over the classical fixed-point iteration.

3.4 THE REGULARIZED SHORT-TERM RECURRENCE ANDERSON MIXING

Inspired by the recent work on stochastic Anderson mixing (SAM) method (Wei et al., 2021), we develop a regularized ST-AM (RST-AM) for solving nonconvex stochastic optimizaiton problems.

Consider the nonconvex optimization problem $\min_{x\in\mathbb{R}^d} f(x) := \frac{1}{T}\sum_{i=1}^{T} f_{\xi_i}(x)$, where $f_{\xi_i} : \mathbb{R}^d \to \mathbb{R}^d$ is the loss function corresponding to i-th data sample and T is the number of data samples. In mini-batch training, the gradient is evaluated as $f_{S_k}(x_k) := \frac{1}{n_k}\sum_{i\in S_k} f_{\xi_i}(x_k)$, where $S_k \subseteq [T] := \{1, 2, \ldots, T\}$ is the sampled mini-batch, and $n_k := |S_k|$ is the batch size. In this case, we set $r_k = -\nabla_{S_k} f(x_k)$ (Line 3 in Algorithm 1), which is an unbiased estimation of the negative gradient.

Recalling from (8), $\zeta_k = (Q_{k-1}^{\mathrm{T}} Q_{k-1})^{\dagger} Q_{k-1}^{\mathrm{T}} \Delta r_{k-1} = \arg\min \|\Delta r_{k-1} - Q_{k-1}\zeta\|_2$ as $q = \Delta r_{k-1}$ by definition. Since ST-AM is based on a local quadratic approximation (5) in a small region around x_k, a large magnitude of $\|P_{k-1}\zeta_k\|_2$ tends to make $p_k = \Delta x_{k-1} - P_{k-1}\zeta_k$ overshoot the trust region around x_k, thus leading to instability. Consequently, we add a penalty term in the above least-square problem, i.e.

$$\zeta_k = \arg\min \|\Delta r_{k-1} - Q_{k-1}\zeta\|_2^2 + \delta_k^{(1)} \|P_{k-1}\zeta\|_2^2, \tag{10}$$

where $\delta_k^{(1)} > 0$. Same as SAM (Wei et al., 2021), we also add a regularization term for computing Γ_k via

$$\Gamma_k = \arg\min \|r_k - Q_k\Gamma\|_2^2 + \delta_k^{(2)} \|P_k\Gamma\|_2^2, \tag{11}$$

where $\delta_k^{(2)} > 0$, and a damping term is used as shown in Line 12 in Algorithm 1. In practice, we choose the two parameters as

$$\delta_k^{(1)} = \frac{c_1\|r_k\|_2^2}{\|\Delta x_{k-1}\|_2^2 + \epsilon_0},\ \delta_k^{(2)} = \max\left\{\frac{c_2\|r_k\|_2^2}{\|p_k\|_2^2 + \epsilon_0}, C\beta_k^{-2}\right\}, \tag{12}$$

where $c_1, c_2, C > 0$ are constants, and $\epsilon_0 > 0$ is a small constant to bound the denominators away from zero. Assume $\|p_{k-1}\|_2 \approx \|p_k\|_2 = \mathcal{O}(\|\Delta x_{k-1}\|_2)$, the choices of (12) make $\|\delta_k^{(1)} P_{k-1}^{\mathrm{T}} P_{k-1}\|_2 \approx \mathcal{O}(\|r_k\|_2^2)$ and $\|\delta_k^{(2)} P_k^{\mathrm{T}} P_k\|_2 \approx \mathcal{O}(\|r_k\|_2^2)$ aware of the change of the local curvature: large (small) $\|r_k\|_2$ tends to lead a large (small) regularization.

Remark 3. *One update of x_k given by Line 11-13 in Algorithm 1 can be formulated as $x_{k+1} = x_k + H_k r_k$, where $H_k = \beta_k I - \alpha_k Y_k Z_k^{\dagger} Q_k^{\mathrm{T}}, Y_k = P_k + \beta_k Q_k, Z_k = Q_k^{\mathrm{T}} Q_k + \delta_k^{(2)} P_k^{\mathrm{T}} P_k$. To guarantee the positive definiteness of H_k, We follow the same procedure in SAM. Let λ_k be the largest eigenvalue of $Y_k Z_k^{\dagger} Q_k^{\mathrm{T}} + Q_k Z_k^{\dagger} Y_k^{\mathrm{T}}$. If α_k satisfies*

$$\alpha_k \lambda_k \leq 2\beta_k(1-\mu), \tag{13}$$

then $s_k^{\mathrm{T}} H_k s_k \geq \beta_k \mu \|s_k\|_2^2, \forall s_k \in \mathbb{R}^d$, where $\mu \in (0,1)$ is a constant. Noted that λ_k can be cheaply obtained by computing the largest eigenvalue of a matrix of $\mathbb{R}^{4\times 4}$ (see Appendix A.3.1).

We summarize the RST-AM in Algorithm 1 and establish its convergence properties in the following context. First, we impose the following assumptions on the objective function f.

Assumption 1. *$f : \mathbb{R}^d \to \mathbb{R}$ is* continuously differentiable. *$f(x) \geq f^{low} > -\infty$ for any $x \in \mathbb{R}^d$. ∇f is globally L-Lipschitz continuous; namely $\|\nabla f(x) - \nabla f(y)\|_2 \leq L\|x-y\|_2$ for any $x, y \in \mathbb{R}^d$.*

Assumption 2. *For any iteration k, the stochastic gradient $\nabla f_{\xi_k}(x_k)$ satisfies $\mathbb{E}_{\xi_k}[\nabla f_{\xi_k}(x_k)] = \nabla f(x_k)$, $\mathbb{E}_{\xi_k}[\|\nabla f_{\xi_k}(x_k) - \nabla f(x_k)\|_2^2] \leq \sigma^2$, where $\sigma > 0$, and $\xi_k, k = 0, 1, \ldots$ are independent samples that are independent of $\{x_j\}_{j=0}^{k}$.*

The diminishing condition about β_k is

$$\sum_{k=0}^{+\infty} \beta_k = +\infty, \sum_{k=0}^{+\infty} \beta_k^2 < +\infty. \tag{14}$$

We give the convergence properties of RST-AM in nonconvex (stochastic) optimization and proofs are deferred to Appendix A.3.2.

Theorem 3. *Suppose Assumption 1 hold and $\{x_k\}$ be the sequence generated by full-batch RST-AM, i.e. $n_k = T$. Let $\beta_k = \beta \in (0, \frac{\mu}{2L(1+C^{-1})}]$ be a constant, $\alpha_k \in [0,1]$ and satisfies (13), then*

$$\frac{1}{N}\sum_{k=0}^{N-1} \|\nabla f(x_k)\|_2^2 \leq \frac{2(f(x_0) - f^{low})}{N\mu\beta}, \tag{15}$$

in the N-th iterations. To ensure $\frac{1}{N}\sum_{k=0}^{N-1} \|\nabla f(x_k)\|_2^2 < \epsilon$, the number of iterations is $\mathcal{O}(1/\epsilon)$.

Theorem 4. *Suppose Assumptions 1 and 2 hold and $\{x_k\}$ be the sequence generated by RST-AM with batch size $n_k = n \leq T$. If $\beta_k \in (0, \frac{\mu}{4L(1+C^{-1})}], \alpha_k \in [0, \min\{1, \beta_k^{\frac{1}{2}}\}]$ and satisfies (13), then*

$$\liminf_{k\to\infty} \|\nabla f(x_k)\|_2 = 0 \text{ with probability } 1 \quad \text{and} \quad \exists M_f > 0 \to \mathbb{E}[f(x_k)] \leq M_f, \forall k. \tag{16}$$

If $\mathbb{E}_{\xi_k}[\|\nabla f_{\xi_k}(x_k)\|_2^2] \leq M_g, \forall k$ where $M_g > 0$ is a constant, we have

$$\lim_{k\to\infty} \|\nabla f(x_k)\|_2 = 0 \text{ with probability } 1. \tag{17}$$

Theorem 5. *Suppose Assumptions 1 and 2 hold and $\{x_k\}_{k=1}^{N}$ be the first N iterations generated by RST-AM with fixed batch size $n_k = n$. Let $\beta_k = \min\{\frac{\mu}{4L(1+C^{-1})}, \frac{\tilde{D}}{\sigma\sqrt{N}}\}$, where $\tilde{D}$ is a problem-independent constant, $\alpha \in [0, \min\{1, \beta_k^{\frac{1}{2}}\}]$ and satisfies (13). Let R be a random variable following $P_R(k) := Prob\{R = k\} = 1/N$, then*

$$\mathbb{E}[\|\nabla f(x_R)\|_2^2] \leq \frac{16 D_f L(1+C^{-1})}{N\mu^2} + \frac{\sigma}{\mu\sqrt{N}}\left(\frac{4D_f}{\tilde{D}} + \frac{4(L+\mu^{-1})(1+C^{-1})\tilde{D}}{n}\right), \tag{18}$$

where $D_f := f(x_0) - f^{low}$ and the expectation is taken with respect to R and $\{S_j\}_{j=0}^{N-1}$. To ensure $\mathbb{E}[\|\nabla f(x_R)\|_2^2] \leq \epsilon$, the number of iterations is $\mathcal{O}(1/\epsilon^2)$.

The proofs of Theorem 4 and Theorem 5 are based on the analysis in SAM (Wei et al., 2021). It is noted that there are two key differences between RST-AM and SAM: RST-AM is more memory efficient; RST-AM has additional correction and regularization term (Line 5-8 in Algorithm 1).

4 EXPERIMENTS

We validate the effectiveness of our proposed ST-AM methods in various applications in fixed-point iterations and nonconvex optimization, including linear and nonlinear problems, deterministic and stochastic optimization. Specifically, we first test ST-AM in solving linear systems and cubic-regularized quadratic minimization (Carmon & Duchi, 2020). Then we apply RST-AM to train neural networks and compare them with several first-order and second-order optimizers. Experimental details and hyperparameter tuning are referred to Appendix B.

4.1 EXPERIMENTS ABOUT THE BASIC ST-AM AND MST-AM

We verify the properties of ST-AM declared in Theorem 1 and Theorem 2 by considering three types of problems (details are in Appendix B.1):
(I) Strongly convex quadratic optimization (cf. (5), corresponding to Theorem 1);
(II) Solving a nonsymmetric linear system $Ax = b$ (corresponding to $\hat{\kappa} = 0$ in Theorem 2);
(III) Cubic-regularized quadratic minimization $\min_{x\in\mathbb{R}^d} f(x) := \|Ax-b\|_2^2 + \frac{M}{3}\|x\|_2^3$ (corresponding to $\hat{\kappa} > 0$ in Theorem 2).

The methods being compared were gradient descent (GD), fixed-point iteration (FP), conjugate residual method (CR) (Saad, 2003), BFGS (Nocedal & Wright, 2006), and the full-memory AM (AM). We used the basic ST-AM to solve Problem I and II, and MST-AM ($c_p = c_q = 1$) to solve Problem III. The target accuracy for convergence was residual $\|r_k\|_2/\|r_0\|_2 \le 1 \times 10^{-15}$.

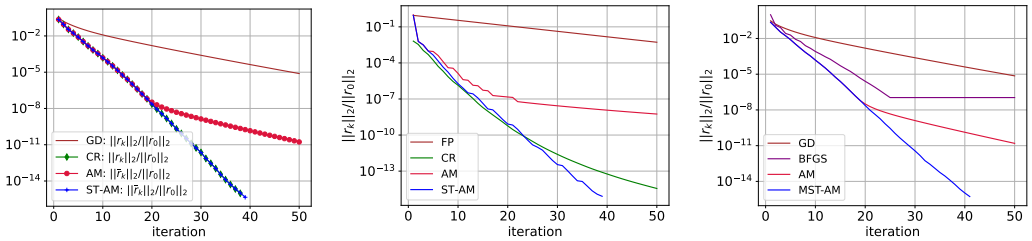

(a) Problem I (b) Probrem II (c) Problem III ($M = 0.1$)

Figure 1: Experiments about ST-AM. (a) The curves of $\|r_k\|_2/\|r_0\|_2$ of GD and CR, and the curves of $\|\bar{r}_k\|_2/\|r_0\|_2$ of AM and ST-AM for solving Problem I; (b) The curves of $\|r_k\|_2/\|r_0\|_2$ for solving Problem II; (c) The curves of $\|r_k\|_2/\|r_0\|_2$ for solving Problem III ($M = 0.1$).

The numerical results shown in Figure 1 demonstrate the power of ST-AM as a variant of Krylov subspace methods. It significantly accelerates the slow convergence of the GD or FP method, and converges faster than AM. Figure 1(a) clearly verifies the correctness of Theorem 1. It can be found that within the machine precision, the intermediate residual $\bar{r}_k$ of ST-AM coincides with the residual r_k of CR. Note that the behaviour of AM does not completely conform to the theory. It fails to coincide with CR and ST-AM due to the intrinsic numerical weakness to solve (3), as also pointed out in (Walker & Ni, 2011). The result in Figure 1(b) shows that ST-AM can outperform CR, though both methods enjoy short-term recurrences and are equivalent for solving SPD linear systems. Since ST-AM has no requirement for the Jacobian or Hessian, it can be applied to more difficult problems. Figure 1(c) shows ST-AM surpasses BFGS in solving cubic-regularized problems.

4.2 EXPERIMENTS ABOUT RST-AM

We apply RST-AM to train neural networks, with full-batch training on MNIST (LeCun et al., 1998), and mini-batch training on CIFAR-10/CIFAR-100 (Krizhevsky et al., 2009), and Penn TreeBank (Marcus et al., 1993).

Experiments on MNIST. We trained a convonlutional neural network (CNN) on MNIST to see the convergence behaviour of RST-AM in nonconvex optimization (cf. Theorem 3), for which we only concerned about the training loss. Figure 2(a)(b) show that the short-memory SAMs ($m = 2, 5$)

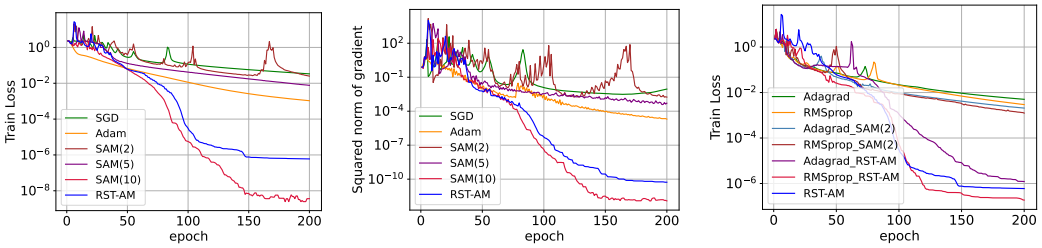

(a) Train loss (w/o preconditioning) (b) SNG (w/o preconditioning) (c) Train loss (w/ preconditioning)

Figure 2: Experiments on MNIST. (a)(b) Training loss and the squared norm of gradient (SNG) (w/o preconditioning for SAM, RST-AM); (c) Training loss (w/ preconditioning for SAM, RST-AM).

hardly show any improvement over the first-order optimizers SGD and Adam, while RST-AM can close the gap of the long-memory ($m = 10$) and the short-memory methods. We also considered the effect of preconditioning on RST-AM (see Appendix B.2). The notation "A_B" means B method preconditioned by A method. Figure 2(c) indicates that preconditioning also works much better for RST-AM than SAM(2), and RMSprop_RST-AM can outperform the non-preconditioned RST-AM.

Table 1: Final TOP1 test accuracy (mean $\pm$ standard deviation) (%) on CIFAR10/CIFAR100.

Method	CIFAR10						CIFAR100		
	ResNet18	ResNet20	ResNet32	ResNet44	ResNet56	WRN16-4	ResNet18	ResNeXt	DenseNet
SGDM	94.82±.15	92.03±.16	92.86±.15	93.10±.23	93.47±.28	94.90±.09	77.27±.09	78.41±.54	78.49±.12
Adam	93.02±.10	91.17±.13	92.03±.28	92.28±.62	92.39±.23	92.45±.11	72.41±.17	73.57±.17	70.23±.54
AdaBound	94.25±.31	90.77±.08	91.73±.06	92.00±.18	92.44±.04	93.50±.12	75.07±.14	75.74±.20	76.06±.13
AdaBelief	94.74±.10	91.15±.21	92.15±.17	92.79±.24	93.30±.07	94.46±.13	76.25±.06	78.27±.16	78.35±.09
Lookahead	94.92±.33	92.07±.04	92.86±.15	93.26±.24	93.36±.13	94.90±.15	77.63±.35	78.93±.12	79.37±.16
AdaHessian	94.36±.09	91.92±.32	92.18±.18	92.74±.11	92.40±.06	94.04±.12	76.59±.42	-	-
SAM(2)	95.07±.04	92.14±.33	93.04±.23	93.46±.09	93.66±.06	95.07±.16	77.51±.24	79.02±.21	80.00±.23
SAM(10)	95.17±.10	**92.43±.19**	93.22±.32	**93.57±.14**	**93.77±.12**	**95.23±.07**	**78.13±.14**	79.31±.27	**80.09±.52**
RST-AM	**95.27±.04**	92.39±.11	**93.24±.36**	93.52±.02	93.69±.18	95.21±.09	77.91±.22	**79.53±.34**	**80.36±.25**

Table 2: The memory and computation cost compared with SGD. Memory, per-epoch time and total running time are abbreviated as "m","t/e" and "t", respectively.

Cost ($\times$ SGD)	CIFAR10/ResNet18			CIFAR10/WRN16-4			CIFAR100/ResNeXt50			CIFAR100/DenseNet121		
	m	t/e	t	m	t/e	t	m	t/e	t	m	t/e	t
SGD	1.00	1.00	1.00	1.00	1.00	1.00	1.00	1.00	1.00	1.00	1.00	1.00
AdaHessian	2.33	5.78	5.78	2.35	5.97	5.97	>1.6	-	-	>1.8	-	-
SAM(10)	1.73	1.78	1.00	1.26	1.28	0.80	1.30	1.16	0.58	1.16	1.19	0.60
RST-AM	1.05	1.46	0.82	1.03	1.14	0.71	1.04	1.07	0.54	1.01	1.11	0.55

Experiments on CIFAR. We trained ResNet18/20/32/44/56 (He et al., 2016), WideResNet16-4 (Zagoruyko & Komodakis, 2016) (abbr. WRN16-4) on CIFAR-10, and ResNet18, ResNeXt50 (Xie et al., 2017), DenseNet121 (Huang et al., 2017) on CIFAR-100. The baseline optimizers were SGDM, Adam, AdaBound (Luo et al., 2019), AdaBelief (Zhuang et al., 2020), Lookahead (Zhang et al., 2019), AdaHessian (Yao et al., 2021) and SAM(10). Table 1 reports the final TOP1 test accuracy for training 160 epochs (AdaHessian ran out of memory for training ResNeXt50, DenseNet121). It shows RST-AM improves SAM(2) and has comparable test accuracy with the long-memory SAM(10). RST-AM also outperforms other baseline optimizers. Table 2 reports the memory and computation cost, where we used SGD as the baseline and other optimizers were terminated when achieving comparable or better test accuracy than SGD. It indicates that RST-AM introduces $\leq 5\%$ extra memory overhead than SGD, and significantly reduces the memory footprint of AM. Since RST-AM needs less training epochs, the total running time is less than SGD.

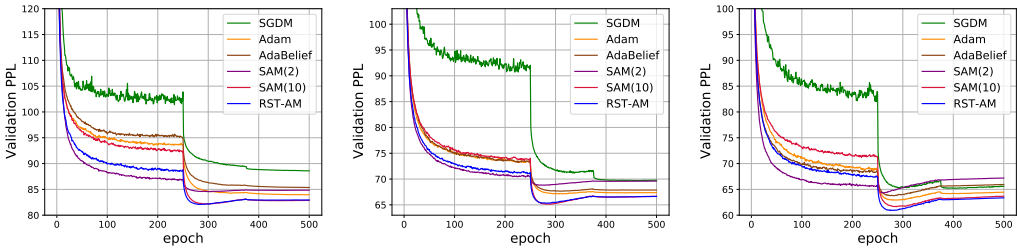

(a) 1-Layer LSTM (b) 2-Layer LSTM (c) 3-Layer LSTM

Figure 3: Experiments on Penn TreeBank. Validation perplexity of training 1,2,3-layer LSTM.

Experiments on Penn TreeBank. We trained LSTMs with 1-3 layers on Penn TreeBank and reported the validation perplexity on Figure 3 and the test perplexity on Table 3 (lower is better). The experimental setting was based on that in AdaBelief. The results show that RST-AM has comparable or even better convergence behaviour than SAM(10). The improvement of RST-AM over other optimizers is also significant. We report the computation and memory cost in Appendix B.2.4. Due to the small batch size, the matrix computation in RST-AM incurs considerable computational overhead. However, RST-AM can still surpass Adam using much less epochs, thus reducing the total running time.

Table 3: Test perplexity on Penn TreeBank for 1,2,3-layer LSTM. Lower is better.

Method	1-Layer	2-Layer	3-Layer
SGDM	83.48±.03	65.89±.18	61.88±.23
Adam	80.33±.15	64.32±.06	59.72±.13
AdaBelief	81.29±.35	64.68±.10	60.46±.07
SAM(2)	80.79±.19	65.52±.29	61.13±.12
SAM(10)	78.78±.14	62.46±.11	58.93±.09
RST-AM	**78.41±.18**	**62.46±.08**	**58.31±.23**

Table 4: Test accuracy (%) for adversarial training.

Optimizer	CIFAR10/ResNet18				CIFAR100/DenseNet121			
	Clean	FGSM	PGD-20	C&W$_\infty$	Clean	FGSM	PGD-20	C&W$_\infty$
SGD	82.16	63.23	51.91	50.22	59.45	39.76	30.92	29.00
RST-AM	82.53	63.78	52.43	50.52	60.48	40.41	31.20	29.52

Experiments on adversarial training. We applied RST-AM to adversarial training (Madry et al., 2018) as the outer-optimizer and compared it with SGD by the clean test accuracy and robust test accuracy. The results on CIFAR10/ResNet18 and CIFAR100/DenseNet121 are reported in Table 4. It can be seen that RST-AM can achieve both higher clean test accuracy and robust test accuracy. More results can be found in Appendix B.2.5.

5 Conclusion

In this paper, to address the memory issue of Anderson mixing (AM), we develop a novel class of short-term recurrence AM methods (ST-AM) and test it on various applications, including solving linear and nonlinear problems, deterministic and stochastic optimization. We give a complete theoretical analysis of the proposed method. We prove that the basic ST-AM is equivalent to the full-memory AM in strongly convex quadratic optimization. With some minor changes, it has local convergence for nonlinear fixed-point iterations under some common assumptions. We also introduce the regularized form of ST-AM and analyze its asymptotic and non-asymptotic convergence properties. The numerical results validate the effectiveness of our method, which show that ST-AM methods are competitive or even better than the long-memory AM while consuming less memory. The regularized ST-AM also outperforms many existing optimizers in training neural networks.

REFERENCES

Hengbin An, Xiaowei Jia, and Homer F Walker. Anderson acceleration and application to the three-temperature energy equations. *Journal of Computational Physics*, 347:1–19, 2017.

Donald G Anderson. Iterative procedures for nonlinear integral equations. *Journal of the ACM (JACM)*, 12(4):547–560, 1965.

Donald GM Anderson. Comments on anderson acceleration, mixing and extrapolation. *Numerical Algorithms*, 80(1):135–234, 2019.

Akash Arora, David C Morse, Frank S Bates, and Kevin D Dorfman. Accelerating self-consistent field theory of block polymers in a variable unit cell. *The Journal of chemical physics*, 146(24): 244902, 2017.

Albert S Berahas, Frank E Curtis, and Baoyu Zhou. Limited-memory bfgs with displacement aggregation. *Mathematical Programming*, pp. 1–37, 2021.

Lon Bottou, Frank E. Curtis, and Jorge Nocedal. Optimization methods for large-scale machine learning. *SIAM Review*, 60(2):223–311, 2018. doi: 10.1137/16M1080173. URL `https://doi.org/10.1137/16M1080173`.

Claude Brezinski and Michela Redivo-Zaglia. Shanks function transformations in a vector space. *Applied Numerical Mathematics*, 116:57–63, 2017.

Claude Brezinski, Michela Redivo-Zaglia, and Yousef Saad. Shanks sequence transformations and anderson acceleration. *SIAM Review*, 60(3):646–669, 2018.

Richard H Byrd, Samantha L Hansen, Jorge Nocedal, and Yoram Singer. A stochastic quasi-newton method for large-scale optimization. *SIAM Journal on Optimization*, 26(2):1008–1031, 2016.

Stan Cabay and LW Jackson. A polynomial extrapolation method for finding limits and antilimits of vector sequences. *SIAM Journal on Numerical Analysis*, 13(5):734–752, 1976.

Nicholas Carlini and David Wagner. Towards evaluating the robustness of neural networks. In *2017 ieee symposium on security and privacy (sp)*, pp. 39–57. IEEE, 2017.

Yair Carmon and John C Duchi. First-order methods for nonconvex quadratic minimization. *SIAM Review*, 62(2):395–436, 2020.

Hans De Sterck and Yunhui He. On the asymptotic linear convergence speed of anderson acceleration, nesterov acceleration, and nonlinear gmres. *SIAM Journal on Scientific Computing*, (0): S21–S46, 2021.

Yunbin Deng. Deep learning on mobile devices: a review. In *Mobile Multimedia/Image Processing, Security, and Applications 2019*, volume 10993, pp. 109930A. International Society for Optics and Photonics, 2019.

John Duchi, Elad Hazan, and Yoram Singer. Adaptive subgradient methods for online learning and stochastic optimization. *Journal of machine learning research*, 12(7), 2011.

Rick Durrett. *Probability: theory and examples*, volume 49. Cambridge university press, 2019.

RP Eddy. Extrapolation to the limit of a vector sequence. information linkage between applied mathematics and industry, pcc wang, 1979.

Claire Evans, Sara Pollock, Leo G Rebholz, and Mengying Xiao. A proof that anderson acceleration improves the convergence rate in linearly converging fixed-point methods (but not in those converging quadratically). *SIAM Journal on Numerical Analysis*, 58(1):788–810, 2020.

Haw-ren Fang and Yousef Saad. Two classes of multisecant methods for nonlinear acceleration. *Numerical Linear Algebra with Applications*, 16(3):197–221, 2009.

Anqi Fu, Junzi Zhang, and Stephen Boyd. Anderson accelerated douglas–rachford splitting. *SIAM Journal on Scientific Computing*, 42(6):A3560–A3583, 2020.

Alejandro J Garza and Gustavo E Scuseria. Comparison of self-consistent field convergence acceleration techniques. *The Journal of chemical physics*, 137(5):054110, 2012.

Ian J Goodfellow, Jonathon Shlens, and Christian Szegedy. Explaining and harnessing adversarial examples. *arXiv preprint arXiv:1412.6572*, 2014.

William W Hager and Hongchao Zhang. A survey of nonlinear conjugate gradient methods. *Pacific journal of Optimization*, 2(1):35–58, 2006.

Kaiming He, Xiangyu Zhang, Shaoqing Ren, and Jian Sun. Deep residual learning for image recognition. In *Proceedings of the IEEE conference on computer vision and pattern recognition*, pp. 770–778, 2016.

Magnus R Hestenes and Eduard Stiefel. Methods of conjugate gradients for solving linear systems1. *Journal cf Research of the National Bureau of Standards Vol*, 49(6), 1952.

Gao Huang, Zhuang Liu, Laurens Van Der Maaten, and Kilian Q Weinberger. Densely connected convolutional networks. In *Proceedings of the IEEE conference on computer vision and pattern recognition*, pp. 4700–4708, 2017.

Carl T Kelley. Numerical methods for nonlinear equations. *Acta Numerica*, 27:207–287, 2018.

Diederik P Kingma and Jimmy Ba. Adam: A method for stochastic optimization. *arXiv preprint arXiv:1412.6980*, 2014.

Tamara G Kolda, Dianne P O'leary, and Larry Nazareth. Bfgs with update skipping and varying memory. *SIAM Journal on Optimization*, 8(4):1060–1083, 1998.

Alex Krizhevsky, Geoffrey Hinton, et al. Learning multiple layers of features from tiny images. 2009.

Yann LeCun, Léon Bottou, Yoshua Bengio, and Patrick Haffner. Gradient-based learning applied to document recognition. *Proceedings of the IEEE*, 86(11):2278–2324, 1998.

Lin Lin, Jianfeng Lu, and Lexing Ying. Numerical methods for kohn–sham density functional theory. *Acta Numerica*, 28:405–539, 2019.

Liangchen Luo, Yuanhao Xiong, Yan Liu, and Xu Sun. Adaptive gradient methods with dynamic bound of learning rate. *arXiv preprint arXiv:1902.09843*, 2019.

Aleksander Madry, Aleksandar Makelov, Ludwig Schmidt, Dimitris Tsipras, and Adrian Vladu. Towards deep learning models resistant to adversarial attacks. In *International Conference on Learning Representations*, 2018.

Vien Mai and Mikael Johansson. Anderson acceleration of proximal gradient methods. In *International Conference on Machine Learning*, pp. 6620–6629. PMLR, 2020.

Mitchell Marcus, Beatrice Santorini, and Mary Ann Marcinkiewicz. Building a large annotated corpus of english: The penn treebank. 1993.

Aryan Mokhtari, Mark Eisen, and Alejandro Ribeiro. Iqn: An incremental quasi-newton method with local superlinear convergence rate. *SIAM Journal on Optimization*, 28(2):1670–1698, 2018.

Ion Necoara, Yu Nesterov, and Francois Glineur. Linear convergence of first order methods for non-strongly convex optimization. *Mathematical Programming*, 175(1):69–107, 2019.

Arkadij Semenovič Nemirovskij and David Borisovich Yudin. Problem complexity and method efficiency in optimization. 1983.

Jorge Nocedal and Stephen Wright. *Numerical optimization*. Springer Science & Business Media, 2006.

Florian A Potra and Hans Engler. A characterization of the behavior of the anderson acceleration on linear problems. *linear Algebra and its Applications*, 438(3):1002–1011, 2013.

Ning Qian. On the momentum term in gradient descent learning algorithms. *Neural networks*, 12 (1):145–151, 1999.

Leslie Rice, Eric Wong, and Zico Kolter. Overfitting in adversarially robust deep learning. In *International Conference on Machine Learning*, pp. 8093–8104. PMLR, 2020.

Herbert Robbins and Sutton Monro. A stochastic approximation method. *The annals of mathematical statistics*, pp. 400–407, 1951.

Youcef Saad and Martin H Schultz. Gmres: A generalized minimal residual algorithm for solving nonsymmetric linear systems. *SIAM Journal on scientific and statistical computing*, 7(3):856–869, 1986.

Yousef Saad. *Iterative methods for sparse linear systems*. SIAM, 2003.

Daniel Shanks. Non-linear transformations of divergent and slowly convergent sequences. *Journal of Mathematics and Physics*, 34(1-4):1–42, 1955.

Tijmen Tieleman and Geoffrey Hinton. Lecture 6.5-rmsprop: Divide the gradient by a running average of its recent magnitude. *COURSERA: Neural networks for machine learning*, 4(2):26–31, 2012.

Alex Toth and CT Kelley. Convergence analysis for anderson acceleration. *SIAM Journal on Numerical Analysis*, 53(2):805–819, 2015.

Henk A Van der Vorst and C Vuik. The superlinear convergence behaviour of gmres. *Journal of computational and applied mathematics*, 48(3):327–341, 1993.

Homer F Walker and Peng Ni. Anderson acceleration for fixed-point iterations. *SIAM Journal on Numerical Analysis*, 49(4):1715–1735, 2011.

Xiao Wang, Shiqian Ma, Donald Goldfarb, and Wei Liu. Stochastic quasi-newton methods for nonconvex stochastic optimization. *SIAM Journal on Optimization*, 27(2):927–956, 2017.

Fuchao Wei, Chenglong Bao, and Yang Liu. Stochastic anderson mixing for nonconvex stochastic optimization. *arXiv preprint arXiv:2110.01543*, 2021.

Peter Wynn. On a device for computing the e m (s n) transformation. *Mathematical Tables and Other Aids to Computation*, pp. 91–96, 1956.

Peter Wynn. Acceleration techniques for iterated vector and matrix problems. *Mathematics of Computation*, 16(79):301–322, 1962.

Saining Xie, Ross Girshick, Piotr Dollár, Zhuowen Tu, and Kaiming He. Aggregated residual transformations for deep neural networks. In *Proceedings of the IEEE conference on computer vision and pattern recognition*, pp. 1492–1500, 2017.

Zhewei Yao, Amir Gholami, Sheng Shen, Mustafa Mustafa, Kurt Keutzer, and Michael Mahoney. Adahessian: An adaptive second order optimizer for machine learning. In *Proceedings of the AAAI Conference on Artificial Intelligence*, volume 35, pp. 10665–10673, 2021.

Sergey Zagoruyko and Nikos Komodakis. Wide residual networks. In *British Machine Vision Conference 2016*. British Machine Vision Association, 2016.

Michael Zhang, James Lucas, Jimmy Ba, and Geoffrey E Hinton. Lookahead optimizer: k steps forward, 1 step back. In *Advances in Neural Information Processing Systems*, pp. 9597–9608, 2019.

Juntang Zhuang, Tommy Tang, Sekhar Tatikonda, Nicha Dvornek, Yifan Ding, Xenophon Papademetris, and James S Duncan. Adabelief optimizer: Adapting stepsizes by the belief in observed gradients. *arXiv preprint arXiv:2010.07468*, 2020.

A PROOFS

We give more details about ST-AM and the proofs of the theorems in the main paper.

A.1 THE BASIC ST-AM FOR STRONGLY CONVEX QUADRATIC OPTIMIZATION

Recall that the strongly convex quadratic optimization is formulated as

$$\min_{x\in\mathbb{R}^d} f(x) := \frac{1}{2}x^{\mathrm{T}}Ax - b^{\mathrm{T}}x, \tag{19}$$

where $A \in \mathbb{R}^{d\times d}$ is SPD, $b \in \mathbb{R}^d$. Solving (19) is equivalent to solving the SPD linear system

$$Ax = b. \tag{20}$$

The detailed basic ST-AM is given as follows.

Algorithm 2 ST-AM for strongly convex quadratic optimization

Input: $x_0 \in \mathbb{R}^d, \beta_k > 0, 0 < max_iter \leq d$.
Output: $x \in \mathbb{R}^d$

$P_0, Q_0 = \mathbf{0} \in \mathbb{R}^{d\times 2}, p_0, q_0 = \mathbf{0} \in \mathbb{R}^d$
for $k = 0, 1, \ldots, max_iter$ **do**
  $r_k = -\nabla f(x_k)$
  if $k > 0$ **then**
    $p = x_k - x_{k-1}, q = r_k - r_{k-1}$ (Compute $\Delta x_{k-1}, \Delta r_{k-1}$)
    $\tilde{q} = q - Q_{k-1}(Q_{k-1}^{\mathrm{T}}q), \tilde{p} = p - P_{k-1}(Q_{k-1}^{\mathrm{T}}q)$ ($\tilde{q} \perp Q_{k-1}$)
    $p_k = \tilde{p}/\|\tilde{q}\|_2, q_k = \tilde{q}/\|\tilde{q}\|_2$ ($\|q_k\|_2 = 1$)
    $P_k = [p_{k-1}, p_k], Q_k = [q_{k-1}, q_k]$ ($Q_k^{\mathrm{T}}Q_k = I_2$)
  end if
  $\Gamma_k = Q_k^{\mathrm{T}}r_k$
  $\bar{x}_k = x_k - P_k\Gamma_k, \bar{r}_k = r_k - Q_k\Gamma_k$ (Projection step: $\bar{r}_k \perp Q_k$)
  $x_{k+1} = \bar{x}_k + \beta_k\bar{r}_k$ (Mixing step)
  if $\|\bar{r}_k\|_2 = 0$ **then**
    break
  end if
end for
return x_k

We first state the relationship of AM with GMRES in the following proposition. Similar results can also be found in (Walker & Ni, 2011).

Let $x_k^{\mathrm{G}}, r_k^{\mathrm{G}} := b - Ax_k^{\mathrm{G}}$ denote the k-th GMRES iterate and residual, respectively, and $\mathcal{K}_k(A, v) := span\{v, Av, \ldots, A^{k-1}v\}$ denotes the k-th Krylov subspace generated by A and v. Define $e^j := (1, 1, \ldots, 1)^{\mathrm{T}} \in \mathbb{R}^j$ for $j \geq 1$. Let $range(X)$ denote the linear space spanned by the columns of X. The main results of the full-memory AM are stated in Proposition 1 and Proposition 2.

Proposition 1 (General linear system)**.** *For solving a general linear system $Ax = b$ with the full-memory AM ($m = k$), suppose that $\beta_k > 0$ and the fixed-point map is $g(x) = (I - A)x + b$. If the initial point of AM is $x_0 = x_0^{\mathrm{G}}$ and $rank(R_k) = m$, then the intermediate iterate $\bar{x}_k$ satisfies $\bar{x}_k = x_k^{\mathrm{G}}$.*

Proof. The definition of the fixed-point map suggests that the residual $r_k = g(x_k) - x_k = b - Ax_k$. Since $R_k = -AX_k$ and A is nonsingular, we have $rank(X_k) = m$. We first show

$$range(X_k) = \mathcal{K}_k(A, r_0^{\mathrm{G}}) \tag{21}$$

by induction. We abbreviate $\mathcal{K}_k(A, r_0^{\mathrm{G}})$ as $\mathcal{K}_k$ in this proof.

First, $\Delta x_0 = \beta_0 r_0 = \beta_0 r_0^{\mathrm{G}}$ since $x_1 = x_0 + \beta_0 r_0$. If $k = 1$, then the proof is complete. Then, suppose that $k > 1$ and, as an inductive hypothesis, that $range(X_{k-1}) = \mathcal{K}_{k-1}$. With (4) we have

$$\begin{aligned}\Delta x_{k-1} &= x_k - x_{k-1} \\ &= \beta_{k-1} r_{k-1} - (X_{k-1} + \beta_{k-1} R_{k-1})\Gamma_{k-1} \\ &= \beta_{k-1}(b - Ax_{k-1}) - (X_{k-1} - \beta_{k-1} A X_{k-1})\Gamma_{k-1} \\ &= \beta_{k-1} b - \beta_{k-1} A(x_0 + \Delta x_0 + \cdots + \Delta x_{k-2}) - (X_{k-1} - \beta_{k-1} A X_{k-1})\Gamma_{k-1} \\ &= \beta_{k-1} r_0 - \beta_{k-1} A X_{k-1} e^{k-1} - (X_{k-1} - \beta_{k-1} A X_{k-1})\Gamma_{k-1}. \end{aligned} \tag{22}$$

Since $r_0 \in \mathcal{K}_{k-1}$, and by the inductive hypothesis $range(X_{k-1}) \subseteq \mathcal{K}_{k-1}$ which also implies $range(AX_{k-1}) \subseteq \mathcal{K}_k$, we know $\Delta x_{k-1} \in \mathcal{K}_k$, which implies $range(X_k) \subseteq \mathcal{K}_k$. Since we assume $rank(X_k) = m = k$ which implies $\dim(range(X_k)) = \dim(\mathcal{K}_k)$, we have $range(X_k) = \mathcal{K}_k$, thus completing the induction. As a result, we also have

$$range(R_k) = range(AX_k) = A\mathcal{K}_k(A, r_0^{\mathrm{G}}). \tag{23}$$

Recalling that to determine Γ_k, we solve the least-squares problem (3) and $R_k = -AX_k$, we have

$$\Gamma_k = \underset{\Gamma \in \mathbb{R}^m}{\arg\min} \|r_k + AX_k\Gamma\|_2. \tag{24}$$

Since $rank(AX_k) = rank(X_k) = m$, (24) has a unique solution. Also, since $r_k = b - Ax_k = b - A(x_0 + X_k e^k) = r_0 - AX_k e^k$, we have $r_k + AX_k\Gamma = r_0 - AX_k e^k + AX_k\Gamma = r_0 - AX_k\tilde{\Gamma}$, where $\tilde{\Gamma} = e^k - \Gamma$. So Γ_k solves (24) if and only if $\tilde{\Gamma}_k = e^k - \Gamma_k$ solves

$$\min_{\tilde{\Gamma} \in \mathbb{R}^m} \|r_0 - AX_k\tilde{\Gamma}\|_2, \tag{25}$$

According to (21), (25) is equal to $\min_{z \in \mathcal{K}_m(A, r_0^{\mathrm{G}})} \|r_0 - Az\|_2$ which is the GMRES minimization problem. Since the solution of (25) is also unique, we have

$$\bar{x}_k = x_k - X_k\Gamma_k = x_k - X_k(e^k - \tilde{\Gamma}_k) = x_0 + X_k\tilde{\Gamma}_k = x_k^{\mathrm{G}}.$$

□

In Proposition 1, the assumption that R_k has full column rank is critical to ensure no stagnation occurs in AM for solving a general linear system. In fact, for SPD linear systems (20) or strongly convex quadratic optimization (19), when AM breaks down, i.e. R_k is rank deficient, AM obtain the exact solution, as shown in the next proposition.

Proposition 2 (SPD)**.** *For applying the full-memory AM to minimize a strongly convex quadratic problem (19), or equivalently, solve a SPD linear system (20), suppose that $\beta_k > 0$ and the fixed-point map is $g(x) = (I - A)x + b$. If $rank(R_k) = k$ holds for $1 \le k < s$ while failing to hold for $k = s$, where $s \ge 1$, then the residual of AM satisfies $r_s = \bar{r}_{s-1} = 0$.*

Proof. The definition of g suggests that the residual $r_k = g(x_k) - x_k = b - Ax_k$. The relation $R_k = -AX_k$ holds during the iterations and the nonsingularity of A implies $rank(X_k) = rank(R_k)$.

For $s = 1$, since the first step of AM is $x_1 = x_0 + \beta_0 r_0$, the assumption $rank(R_1) = 0$ implies that $rank(r_0) = rank(X_1) = 0$, i.e. $\bar{r}_0 := r_0 = 0$.

For $s > 1$, because $\Delta x_{s-1} = x_s - x_{s-1} = -X_{s-1}\Gamma_{s-1} + \beta_{s-1}\bar{r}_{s-1}$, the rank deficiency of X_s implies $\Delta x_{s-1} \in range(X_{s-1})$, which further implies $\bar{r}_{s-1} \in range(X_{s-1})$. So there exists $\zeta \in \mathbb{R}^{s-1}$, such that $\bar{r}_{s-1} = X_{s-1}\zeta$. Note that according to (3), $\bar{r}_{s-1} \perp R_{s-1} = -AX_{s-1}$, so we have

$$0 = \bar{r}_{s-1}^{\mathrm{T}} A X_{s-1} = (X_{s-1}\zeta)^{\mathrm{T}} A X_{s-1} = \zeta^{\mathrm{T}} X_{s-1}^{\mathrm{T}} A X_{s-1}. \tag{26}$$

Because $rank(X_{s-1}) = s - 1$ and A is SPD, we know $X_{s-1}^{\mathrm{T}} A X_{s-1}$ is also SPD. So $\zeta = 0$, which implies $\bar{r}_{s-1} = 0$. Hence $x_s = \bar{x}_{s-1}$ and $r_s = \bar{r}_{s-1} = 0$. □

Now we give the proof of Theorem 1.

Proof of Theorem 1. Besides relations (i)-(iii), we add an auxiliary relation here:
(iv) $r_k = r_0 + \bar{Q}_k \bar{\Gamma}_k \in \mathcal{K}_{k+1}(A, r_0)$, where $\bar{\Gamma}_k \in \mathbb{R}^k$.
We prove the relations (i)-(iv) by induction.

For $k = 1$, since $\bar{r}_0 \neq 0$, according to Proposition 2, $rank(\Delta x_0) = rank(X_1) = 1, rank(\Delta r_0) = rank(R_1) = 1$, so $\tilde{q} \neq 0$, which implies Line 7 in Algorithm 2 is well-defined. The relation (i) holds. Since $\tilde{q} = q = \Delta x_0, \tilde{p} = p = \Delta r_0$, and $\Delta r_0 = -A\Delta x_0$, the equality $\bar{Q}_1 = -A\bar{P}_1$ also holds. Due to the normalization in Line 7, $\bar{Q}_1^{\mathrm{T}}\bar{Q}_1 = 1$. Since $r_1 = r_0 - \beta_0 A r_0$ and $range(\bar{Q}_1) = range(Ar_0)$, it is clear that $r_1 = r_0 - \bar{Q}_1\bar{\Gamma}_1 \in \mathcal{K}_2(A, r_0)$, namely relation (iv). Due to the projection step Line 11, $\bar{r}_1 \perp range(Q_1) = range(\bar{Q}_1)$. Also, $\bar{r}_1 = r_1 - Q_1\Gamma_1 = r_0 - \beta_0 A r_0 - Q_1\Gamma_1 = r_0 - \bar{Q}_1\eta_1$, where the last equality is due to $span\{Ar_0\} = range(Q_1) = range(\bar{Q}_1)$. For $r_1^{\mathrm{G}} = r_0 - Az_1$, where $z_1 = \arg\min_{z \in \mathcal{K}_1(A, r_0)} \|r_0 - Az\|_2$, it holds $r_1^{\mathrm{G}} \perp A\mathcal{K}_1(A, r_0) = range(\bar{Q}_1)$. As a result, both $\bar{r}_1$ and r_1^{G} are the orthogonal projections of r_0 onto the subspace $\bar{Q}_1^{\perp}$, which implies $\bar{r}_1 = r_1^{\mathrm{G}}$. So $\bar{x}_1 = x_1^{\mathrm{G}} = x_0 + z_1$ because their residuals are equal and A is nonsingular. Hence relation (iii) holds.

Suppose that $k > 1$, and as an inductive hypothesis, the relations (i)-(iv) hold for $j = 1, \ldots, k-1$. Consider the k-th iteration. From Line 6 in Algorithm 2, $\tilde{q} \in range(\Delta r_{k-1}, Q_{k-1})$, and $\tilde{p} \in range(\Delta x_{k-1}, P_{k-1})$. We first prove that $\tilde{q} \neq 0$ by contradiction.

If $\tilde{q} = 0$, then from Line 6 in Algorithm 2, $\Delta r_{k-1} \in range(Q_{k-1}) \subseteq range(\bar{Q}_{k-1})$, which implies $\Delta x_{k-1} \in range(P_{k-1}) \subseteq range(\bar{P}_{k-1})$ as $\Delta r_{k-1} = -A\Delta x_{k-1}$ and $\bar{Q}_{k-1} = -A\bar{P}_{k-1}$ and A is nonsingular. From Line 11 and Line 12, we have

$$\Delta x_{k-1} = x_k - x_{k-1} = -P_{k-1}\Gamma_{k-1} + \beta_{k-1}\bar{r}_{k-1}. \tag{27}$$

So $\bar{r}_{k-1} \in range(P_{k-1}) \subseteq range(\bar{P}_{k-1})$ since $\Delta x_{k-1} \in range(P_{k-1})$. Hence there exists $\zeta \in \mathbb{R}^{k-1}$, such that $\bar{r}_{k-1} = \bar{P}_{k-1}\zeta$. From the inductive hypothesis, we know $\bar{r}_{k-1} \perp \bar{Q}_{k-1} = -A\bar{P}_{k-1}$, so we have

$$0 = \bar{r}_{k-1}^{\mathrm{T}} A\bar{P}_{k-1} = (\bar{P}_{k-1}\zeta)^{\mathrm{T}} A\bar{P}_{k-1} = \zeta^{\mathrm{T}}\bar{P}_{k-1}^{\mathrm{T}} A\bar{P}_{k-1}.$$

Since $\bar{Q}_{k-1}^{\mathrm{T}}\bar{Q}_{k-1} = I_{k-1}$, we know $rank(\bar{Q}_{k-1}) = k-1$, which implies $rank(\bar{P}_{k-1}) = k-1$ due to $\bar{Q}_{k-1} = -A\bar{P}_{k-1}$. Hence $\bar{P}_{k-1}^{\mathrm{T}} A\bar{P}_{k-1}$ is also SPD. Then $\zeta = 0$ which implies $\bar{r}_{k-1} = 0$. It is impossible otherwise Algorithm 2 has terminated in the $(k-1)$-th iteration. So $\tilde{q} \neq 0$ and Line 7 is well-defined.

Since $\bar{r}_{k-1} = r_{k-1} - Q_{k-1}\Gamma_{k-1}$, and $r_{k-1} \in \mathcal{K}_k(A, r_0), range(Q_{k-1}) \subseteq range(\bar{Q}_{k-1}) = A\mathcal{K}_{k-1}(A, r_0)$ as the inductive hypothesis, we have $\bar{r}_{k-1} \in \mathcal{K}_k(A, r_0)$, which together with (27) and $range(P_{k-1}) \subseteq range(\bar{P}_{k-1}) = \mathcal{K}_{k-1}(A, r_0)$ infers $\Delta x_{k-1} \in \mathcal{K}_k(A, r_0)$. Hence $\Delta r_{k-1} = -A\Delta x_{k-1} \in A\mathcal{K}_k(A, r_0)$. As a result, $q_k = \tilde{q}/\|\tilde{q}\|_2 \in range(\Delta r_{k-1}, Q_{k-1}) \subseteq A\mathcal{K}_k(A, r_0)$. So $range(\bar{Q}_k) = range(\bar{Q}_{k-1}, q_k) \subseteq A\mathcal{K}_k(A, r_0)$. Moreover, $q_k \notin \bar{Q}_{k-1}$, otherwise $\tilde{q} \in range(\bar{Q}_{k-1})$ that implies $\Delta r_{k-1} = g \in range(\bar{Q}_{k-1})$, which is impossible following the former proof of $\tilde{q} \neq 0$. So we have $range(\bar{Q}_k) = A\mathcal{K}_k(A, r_0)$.

Because $\Delta r_{k-1} = -A\Delta x_{k-1}$ and $Q_{k-1} = -AP_{k-1}$ due to $\bar{Q}_{k-1} = -A\bar{P}_{k-1}$, Line 6 in Algorithm 2 infers $\tilde{q} = -A\tilde{p}$, which implies $q_k = -Ap_k$. So $\bar{Q}_k = -A\bar{P}_k$. Since A is nonsingular and $range(\bar{Q}_k) = A\mathcal{K}_k(A, r_0)$, we have $\bar{P}_k = \mathcal{K}_k(A, r_0)$.

As $range(X_k) = \mathcal{K}_k(A, r_0)$ and $range(R_k) = A\mathcal{K}_k(A, r_0)$ has been proved in Proposition 1, the relation (i) holds for the k-th iteration.

To prove $\bar{Q}_k^{\mathrm{T}}\bar{Q}_k = I_k$, it suffices to show $q_k \perp \bar{Q}_{k-1}$, as the equalities $\bar{Q}_{k-1}^{\mathrm{T}}\bar{Q}_{k-1} = I_{k-1}$ and $\|q_k\|_2 = 1$ has already held. It is equivalent to prove $\tilde{q} \perp \bar{Q}_{k-1}$. From the construction of $\tilde{q}$ in Line 6 in Algorithm 2, we know $Q_{k-1}^{\mathrm{T}}\tilde{q} = 0$, so $\tilde{q} \perp span(q_{k-2}, q_{k-1})$ (for $k = 2$, $\tilde{q} \perp q_0 = \mathbf{0}$ clearly holds). To further prove $\tilde{q} \perp range(\bar{Q}_{k-3})(k \geq 4)$, note that

$$\Delta r_{k-1} = -A\Delta x_{k-1} = AP_{k-1}\Gamma_{k-1} - \beta_{k-1}A\bar{r}_{k-1} = -Q_{k-1}\Gamma_{k-1} - \beta_{k-1}A\bar{r}_{k-1},$$

where the second equality is a direct substitution with (27). Therefore,

$$\bar{Q}_{k-3}^{\mathrm{T}}\Delta r_{k-1} = -\bar{Q}_{k-3}^{\mathrm{T}}Q_{k-1}\Gamma_{k-1} - \beta_{k-1}\bar{Q}_{k-3}^{\mathrm{T}}A\bar{r}_{k-1} = 0 - \beta_{k-1}(A\bar{Q}_{k-3})^{\mathrm{T}}\bar{r}_{k-1} = 0, \tag{28}$$

where the second equality is due to $range(Q_{k-1}) = span(q_{k-2}, q_{k-1}) \perp range(\bar{Q}_{k-3})$ and A is SPD, the third equality is due to $\bar{r}_{k-1} \perp range(\bar{Q}_{k-1}) = A\mathcal{K}_{k-1}(A, r_0)$ and $range(A\bar{Q}_{k-3}) =$

$A^2\mathcal{K}_{k-3}(A, r_0) \subseteq A\mathcal{K}_{k-1}(A, r_0)$. As a result, noting that $q = \Delta r_{k-1}$, we obtain

$$\bar{Q}_{k-3}^{\mathrm{T}}\tilde{q} = \bar{Q}_{k-3}^{\mathrm{T}}q - \bar{Q}_{k-3}^{\mathrm{T}}Q_{k-1}(Q_{k-1}^{\mathrm{T}}q) = 0,$$

which is due to (28) and $range(Q_{k-1}) = span\{q_{k-2}, q_{k-1}\} \perp range(\bar{Q}_{k-3})$. Therefore, we show that $\bar{Q}_k^{\mathrm{T}}\bar{Q} = I_k$, which along with $\bar{Q}_k = -A\bar{P}_k$ proves relation (ii) in the k-th iteration.

Next, we prove the relation (iv). Since

$$\begin{aligned} r_k &= \bar{r}_{k-1} - \beta_{k-1}A\bar{r}_{k-1} \\ &= r_{k-1} - Q_{k-1}\Gamma_{k-1} - \beta_{k-1}A(r_{k-1} - Q_{k-1}\Gamma_{k-1}) \\ &= r_{k-1} - Q_{k-1}\Gamma_{k-1} - \beta_{k-1}Ar_{k-1} + \beta_{k-1}AQ_{k-1}\Gamma_{k-1} \\ &= r_0 + \bar{Q}_{k-1}\bar{\Gamma}_{k-1} - Q_{k-1}\Gamma_{k-1} - \beta_{k-1}(Ar_0 + A\bar{Q}_{k-1}\bar{\Gamma}_{k-1}) + \beta_{k-1}AQ_{k-1}\Gamma_{k-1}, \end{aligned}$$

where the last equality is due to $r_{k-1} = r_0 + \bar{Q}_{k-1}\bar{\Gamma}_{k-1}$ by the inductive hypothesis. Since $range(\bar{Q}_{k-1}) = A\mathcal{K}_{k-1}(A, r_0) \subseteq A\mathcal{K}_k(A, r_0), range(Q_{k-1}) \subseteq range(\bar{Q}_k), span\{Ar_0\} \in A\mathcal{K}_k(A, r_0), range(AQ_{k-1}) \subseteq range(A\bar{Q}_{k-1}) \subseteq A^2\mathcal{K}_{k-1}(A, r_0) \subseteq A\mathcal{K}_k(A, r_0)$, and $range(\bar{Q}_k) = A\mathcal{K}_k(A, r_0)$, it is clear that $r_k = r_0 + \bar{Q}_k\bar{\Gamma}_k \in \mathcal{K}_{k+1}(A, r_0)$ for some $\bar{\Gamma}_k \in \mathbb{R}^k$. The relation (iv) is proved.

Finally, we prove the relation (iii). For proving $\bar{r}_k \perp range(\bar{Q}_k)$, note that $\bar{r}_k \perp span\{q_{k-1}, q_k\} = range(Q_k)$ already holds due to the projection step (Line 10 and Line 11 in Algorithm 2). It suffices to prove $\bar{r}_k \perp range(\bar{Q}_{k-2})$. In fact, since we have $\bar{r}_k = r_k - Q_k\Gamma_k$, we can prove that $r_k \perp range(\bar{Q}_{k-2})$ and $Q_k\Gamma_k \perp range(\bar{Q}_{k-2})$:

Since $range(Q_k) = span\{q_{k-1}, q_k\} \perp range(\bar{Q}_{k-2})$ as induced from $\bar{Q}_k^{\mathrm{T}}\bar{Q}_k = I_k$, it is clear that $Q_k\Gamma_k \perp range(\bar{Q}_{k-2})$. For r_k, according to Line 12 in Algorithm 2, we have $r_k = \bar{r}_{k-1} - \beta_{k-1}A\bar{r}_{k-1}$. We have $\bar{r}_{k-1} \perp range(\bar{Q}_{k-1}) \supseteq range(\bar{Q}_{k-2})$ by the inductive hypothesis. Also, $\bar{Q}_{k-2}^{\mathrm{T}}A\bar{r}_{k-1} = (A\bar{Q}_{k-2})^{\mathrm{T}}\bar{r}_{k-1} = 0$ due to $range(A\bar{Q}_{k-2}) = A^2\mathcal{K}_{k-2}(A, r_0) \subseteq A\mathcal{K}_{k-1}(A, r_0) = range(\bar{Q}_{k-1})$.

Therefore, we obtain $\bar{r}_k \perp range(\bar{Q}_{k-2})$, which along with $\bar{r}_k \perp span\{q_{k-1}, q_k\}$ implies $\bar{r}_k \perp range(\bar{Q}_k)$.

To prove $\bar{x}_k = x_k^{\mathrm{G}} := x_0 + z_k$, where $z_k = \arg\min_{z \in \mathcal{K}_k(A, r_0)} \|r_0 - Az\|_2$, first we have $r_k = r_0 + \bar{Q}_k\bar{\Gamma}_k$, where $\bar{\Gamma}_k \in \mathbb{R}^k$. Hence $\bar{r}_k = r_k - Q_k\Gamma_k = r_0 - \bar{Q}_k\bar{\Gamma}_k - Q_k\Gamma_k = r_0 - \bar{Q}_k\eta_k$, where $\eta_k \in \mathbb{R}^k$. Since $\bar{r}_k \perp \bar{Q}_k$, $\bar{r}_k$ is the orthogonal projection of r_0 onto the subspace $range(\bar{Q}_k)^{\perp}$. On the other side, for GMRES, $r_k^{\mathrm{G}} = r_0 - Az_k \perp A\mathcal{K}_k(A, r_0) = range(\bar{Q}_k)$, so r_k^{G} is also the orthogonal projection of r_0 onto the subspace $range(\bar{Q}_k)^{\perp}$. So $\bar{r}_k = r_k^{\mathrm{G}}$, which further indicates $\bar{x}_k = x_k^{\mathrm{G}}$. Hence, the relation (iii) holds.

With relations (i)-(iv) being proved in the k-th iteration, we complete the induction. □

A.2 Modified ST-AM for general fixed-point iterations

Algorithm 2 is suitable for analysis and implementation in the linear case. For general nonlinear fixed-point iterations, we adopt an alternative form as described in Algorithm 3 which discards the normalization of $\tilde{q}$ in each iteration (Line 7 in Algorithm 2). In Line 7 in Algorithm 3, the orthogonal projection of Δr_{k-1} is checked to ensure Δr_{k-1} is "less linearly dependent" on $range(Q_k)$, which ensures $\|q_k\|_2$ is bounded away from zero; the check of $\|P_{k-1}\zeta_k\|_2$ ensures that $\|p_k - \Delta x_{k-1}\|_2 < c_p\|\Delta x_{k-1}\|_2$, which is also important since a large deviation from Δx_{k-1} can make $\|p_k\|_2 > \rho$ (ρ is the radius introduced in Theorem 2). When this condition cannot be satisfied, the algorithm simply reuses the old P_{k-1}, Q_{k-1}. The main procedure of LST-AM restarts every m iterations, i.e. $P_k, Q_k = \mathbf{0}$. Such restart mechanism is to restrict the higher-order terms in the residual expansion, as shown in (9). Also, restart can flush out the outdated historical information that may weaken the quality of P_k and Q_k that are used to pursue a local first-order approximation of g in LST-AM.

In the linear case, Algorithm 2 and Algorithm 3 (with $m = \infty$) are equivalent. Similar to Algorithm 2, we have the following properties held for restarted LST-AM:

Claim 1. *In the k-th iteration ($k > 0$) of Algorithm 1 applied to minimize a strongly convex quadratic problem (5), assuming $c_p = \infty, c_q = 1, m = \infty$, the following relation hold:*

Algorithm 3 MST-AM for nonlinear fixed-point problems

Input: $x_0 \in \mathbb{R}^d, \beta_k \in (0,1], c_p > 0, c_q \in (0,1], m > 0.$
Output: $x \in \mathbb{R}^d$

1: $P_0, Q_0 = \mathbf{0} \in \mathbb{R}^{d\times 2}, p_0, q_0 = \mathbf{0} \in \mathbb{R}^d$
2: **for** $k = 0, 1, \ldots,$ until convergence **do**
3: $\quad r_k = g(x_k) - x_k$
4: $\quad$ **if** $k \mod m \neq 0$ **then**
5: $\quad\quad p = x_k - x_{k-1}, q = r_k - r_{k-1}$
6: $\quad\quad \zeta_k = (Q_{k-1}^{\mathrm{T}} Q_{k-1})^{\dagger} Q_{k-1}^{\mathrm{T}} q$
7: $\quad\quad$ **if** $\|P_{k-1}\zeta_k\|_2 < c_p\|p\|_2$ and $\|Q_{k-1}\zeta_k\|_2 < c_q\|q\|_2$ **then**
8: $\quad\quad\quad p_k = p - P_{k-1}\zeta_k, q_k = q - Q_{k-1}\zeta_k$
9: $\quad\quad\quad P_k = [p_{k-1}, p_k], Q_k = [q_{k-1}, q_k]$ $\quad$ $(q_k \perp Q_{k-1})$
10: $\quad\quad$ **else**
11: $\quad\quad\quad P_k = P_{k-1}, Q_k = Q_{k-1}$
12: $\quad\quad$ **end if**
13: $\quad$ **else**
14: $\quad\quad P_k, Q_k = \mathbf{0} \in \mathbb{R}^{d\times 2}, p_k, q_k = \mathbf{0} \in \mathbb{R}^d$
15: $\quad$ **end if**
16: $\quad \Gamma_k = (Q_k^{\mathrm{T}} Q_k)^{\dagger} Q_k^{\mathrm{T}} r_k$
17: $\quad \bar{x}_k = x_k - P_k\Gamma_k, \bar{r}_k = r_k - Q_k\Gamma_k$ $\quad$ (Projection step: $\bar{r}_k \perp Q_k$)
18: $\quad x_{k+1} = \bar{x}_k + \beta_k \bar{r}_k$ $\quad$ (Mixing step)
19: **end for**
20: **return** x_k

(The notation "†" is the Moore-Penrose pseudoinverse.)

(i) $\|q_k\|_2 > 0, range(\bar{P}_k) = range(X_k) = \mathcal{K}_k(A, r_0), range(\bar{Q}_k) = range(R_k) = A\mathcal{K}_k(A, r_0)$*;*
(ii) $\bar{Q}_k = -A\bar{P}_k$*,* $q_i \perp q_j (1 \leq i \neq j \leq k)$*;*
(iii) $\bar{r}_k \perp range(\bar{Q}_k)$ *and* $\bar{x}_k = x_0 + z_k$*, where* $z_k = \arg\min_{z\in\mathcal{K}_k(A,r_0)} \|r_0 - Az\|_2$*.*
If $\|\bar{r}_k\|_2 = 0$*, then* x_{k+1} *is the exact solution.*

The proof of Claim 1 is essentially the same as the proof of Theorem 1, with a special care that $\bar{Q}_k^{\mathrm{T}}\bar{Q}_k = I_k$ is replaced by the relation that columns of $\bar{Q}_k$ are orthogonal to each other, in other words, $\bar{Q}_k^{\mathrm{T}}\bar{Q}_k = diag\{\|q_1\|_2^2, \ldots, \|q_k\|_2^2\}$.

For minimizing nonlinear functions or accelerating nonlinear fixed-point iterations, the long-term relation that $\bar{Q}_k^{\mathrm{T}}\bar{Q}_k = diag\{\|q_1\|_2^2, \ldots, \|q_k\|_2^2\}$ generally cannot hold, while the orthogonalization procedure in Line 6 still leads to a short-term orthogonalization relation: $q_i \perp q_j$ for $|i - j| \leq 2$. Hence, $Q_k^{\mathrm{T}} Q_k = diag\{\|q_{k-1}\|_2^2, \|q_k\|_2^2\}$ for $k \geq 1$. Thus the pseudoinverse $(Q_k^{\mathrm{T}} Q_k)^{\dagger} = diag\{\mathcal{I}(\|q_k\|_2 \neq 0)1/\|q_k\|_2^2, \mathcal{I}(\|q_k\|_2 \neq 0)1/\|q_k\|_2^2\}$, where $\mathcal{I}(\cdot)$ is the indicator function that

$$\mathcal{I}(x) = \begin{cases} 1 & x \text{ is true,} \\ 0 & x \text{ is false.} \end{cases}$$

Now, we give the proof of Theorem 2.

Proof. For convenience, we restate the main assumptions of g here:

$$\text{(i) } \|g(y) - g(x)\|_2 \leq \kappa\|y - x\|_2, \text{ for } \forall x, y \in \mathcal{B}(\rho), \tag{29a}$$

$$\text{(ii) } \|g'(y) - g'(x)\|_2 \leq \hat{\kappa}\|y - x\|_2, \text{ for } \forall x, y \in \mathcal{B}(\rho). \tag{29b}$$

The proof is based on the two lemmas given in Lemma 1 and Lemma 2. With (42a), we know if $\|r_k\|_2$ is small, then $\|x_k - x^*\|_2$ is small as well. Hence we can always ensure $x_k \in \mathcal{B}(\rho)$ if we choose $\|x_0 - x^*\|_2$ to be sufficiently small and $\|r_k\|_2$ is non-increasing during the iterations.

At the end of the k-th iteration of Algorithm 3, we have

$$\begin{aligned} r_{k+1} &= g(x_{k+1}) - x_{k+1} \\ &= g(x_{k+1}) - g(\bar{x}_k) + g(\bar{x}_k) - (\bar{x}_k + \beta_k \bar{r}_k) \\ &= (g(x_{k+1}) - g(\bar{x}_k)) + (g(\bar{x}_k) - \bar{x}_k - \bar{r}_k) + (1-\beta_k)\bar{r}_k. \end{aligned} \tag{30}$$

Let $\mathcal{L}_k := g(x_{k+1}) - g(\bar{x}_k) + (1-\beta_k)\bar{r}_k$, $\mathcal{H}_k := g(\bar{x}_k) - \bar{x}_k - \bar{r}_k$, then

$$\begin{aligned} \|\mathcal{L}_k\|_2 &\leq \kappa \|x_{k+1} - \bar{x}_k\|_2 + |1-\beta_k| \|\bar{r}_k\|_2 \\ &= \kappa \beta_k \|\bar{r}_k\|_2 + |1-\beta_k| \|\bar{r}_k\|_2 \\ &= \theta_k (\kappa \beta_k + |1-\beta_k|) \|r_k\|_2, \end{aligned} \tag{31}$$

which bounds the linear part of the residual r_{k+1}.

For the higher-order terms $\mathcal{H}_k$, we have

$$\begin{aligned} \mathcal{H}_k &= g(\bar{x}_k) - (x_k - P_k \Gamma_k + r_k - Q_k \Gamma_k) \\ &= g(\bar{x}_k) - g(x_k) + (P_k + Q_k)\Gamma_k. \\ &= g(\bar{x}_k) - g(x_k) + (p_k + q_k)\gamma_k^{(2)} + (p_{k-1} + q_{k-1})\gamma_k^{(1)}, \end{aligned} \tag{32}$$

where $\Gamma_k = (\gamma_k^{(1)}, \gamma_k^{(2)})^{\mathrm{T}} \in \mathbb{R}^2$. Since $\Gamma_k = (Q_k^{\mathrm{T}} Q_k)^{\dagger} Q_k^{\mathrm{T}} r_k$, $Q_k^{\mathrm{T}} Q_k = diag\{\|q_{k-1}\|_2^2, \|q_k\|_2^2\}$, it follows that

$$\gamma_k^{(1)} = \mathcal{I}(q_{k-1} \neq 0) \frac{r_k^{\mathrm{T}} q_{k-1}}{q_{k-1}^{\mathrm{T}} q_{k-1}},\ \gamma_k^{(2)} = \mathcal{I}(q_k \neq 0) \frac{r_k^{\mathrm{T}} q_k}{q_k^{\mathrm{T}} q_k}. \tag{33}$$

Therefore,

$$\begin{aligned} &|\gamma_k^{(1)}| \leq \mathcal{I}(q_{k-1} \neq 0) \frac{\|r_k\|_2}{\|q_{k-1}\|_2},\ |1-\gamma_k^{(1)}| \leq \mathcal{I}(q_{k-1} \neq 0) \frac{\|r_k - q_{k-1}\|_2}{\|q_{k-1}\|_2}, \\ &|\gamma_k^{(2)}| \leq \mathcal{I}(q_k \neq 0) \frac{\|r_k\|_2}{\|q_k\|_2},\ |1-\gamma_k^{(2)}| \leq \mathcal{I}(q_k \neq 0) \frac{\|r_k - q_k\|_2}{\|q_k\|_2} \end{aligned} \tag{34}$$

According to the formula $\int_0^1 g'(x + t(y-x))(y-x)dt = g(y) - g(x)$, we have

$$\begin{aligned} g(\bar{x}_k) - g(x_k) &= g(\bar{x}_k) - g(x_k - p_k \gamma_k^{(2)}) + g(x_k - p_k \gamma_k^{(2)}) - g(x_k) \\ &= \int_0^1 -g'(x_k - p_k \gamma_k^{(2)} - t p_{k-1} \gamma_k^{(1)}) p_{k-1} \gamma_k^{(1)} dt \\ &\quad + \int_0^1 -g'(x_k - t p_k \gamma_k^{(2)}) p_k \gamma_k^{(2)} dt. \end{aligned} \tag{35}$$

Also, by Lemma 2, we have

$$p_k + q_k = \int_0^1 g'(x_k - t p_k) p_k dt + \hat{\kappa} \|\Delta r_{\pi(k)-1}\|_2 \sum_{j=k-m_k}^{k-1} \mathcal{O}(\|\Delta r_j\|_2),$$

$$p_{k-1} + q_{k-1} = \int_0^1 g'(x_{k-1} - t p_{k-1}) p_{k-1} dt + \hat{\kappa} \|\Delta r_{\upsilon(k)-1}\|_2 \sum_{j=k-m_k}^{k-2} \mathcal{O}(\|\Delta r_j\|_2),$$

where $\pi(k)$ denotes that the latest update of q_k by Line 8 occurs in the $\pi(k)$-th iteration and $\upsilon(k) = \pi(\pi(k)-1)$ marks that q_{k-1} records $q_{\upsilon(k)}$ that is the latest update by Line 8 occurred in the $\upsilon(k)$-th iteration.

By substituting these relations to (32), it follows that

$$
\begin{aligned}
\mathcal{H}_k &= \left(\int_0^1 g'(x_k - tp_k)p_k dt + \hat{\kappa}\|\Delta r_{\pi(k)-1}\|_2 \sum_{j=k-m_k}^{k-1} \mathcal{O}(\|\Delta r_j\|_2) \right) \gamma_k^{(2)} \\
&\quad + \left(\int_0^1 g'(x_{k-1} - tp_{k-1})p_{k-1} dt + \hat{\kappa}\|\Delta r_{\upsilon(k)-1}\|_2 \sum_{j=k-m_k}^{k-2} \mathcal{O}(\|\Delta r_j\|_2) \right) \gamma_k^{(1)} \\
&\quad - \int_0^1 g'(x_k - p_k\gamma_k^{(2)} - tp_{k-1}\gamma_k^{(1)})p_{k-1}\gamma_k^{(1)} dt - \int_0^1 g'(x_k - tp_k\gamma_k^{(2)})p_k\gamma_k^{(2)} dt \\
&= \int_0^1 (g'(x_k - tp_k) - g'(x_k - tp_k\gamma_k^{(2)}))p_k\gamma_k^{(2)} dt \\
&\quad + \int_0^1 (g'(x_{k-1} - tp_{k-1}) - g'(x_k - p_k\gamma_k^{(2)} - tp_{k-1}\gamma_k^{(1)}))p_{k-1}\gamma_k^{(1)} dt \\
&\quad + \hat{\kappa}\|\Delta r_{\pi(k)-1}\|_2 \sum_{j=k-m_k}^{k-1} \mathcal{O}(\|\Delta r_j\|_2)\gamma_k^{(2)} \\
&\quad + \hat{\kappa}\|\Delta r_{\upsilon(k)-1}\|_2 \sum_{j=k-m_k}^{k-2} \mathcal{O}(\|\Delta r_j\|_2)\gamma_k^{(1)} \\
&= A_k + B_k + C_k + D_k. \qquad (36)
\end{aligned}
$$

Then we can bound each terms of $\mathcal{H}_k$ as follows (Here we assume $q_k \neq 0$ and $q_{k-1} \neq 0$ as $q_k = 0$ leads to $\gamma_k^{(2)} = 0$ and $q_{k-1} = 0$ leads to $\gamma_k^{(1)} = 0$ where the result is trivial.):

$$
\begin{aligned}
\|A_k\|_2 &= \left\| \int_0^1 (g'(x_k - tp_k) - g'(x_k - tp_k\gamma_k^{(2)}))p_k\gamma_k^{(2)} dt \right\|_2 \\
&\leq \int_0^1 \|g'(x_k - tp_k) - g'(x_k - tp_k\gamma_k^{(2)})\|_2 \|p_k\gamma_k^{(2)}\|_2 dt \\
&\leq \hat{\kappa} \int_0^1 \|tp_k - tp_k\gamma_k^{(2)}\|_2 \|p_k\|_2 |\gamma_k^{(2)}| dt \\
&= \frac{\hat{\kappa}}{2}\|p_k\|_2^2 |1 - \gamma_k^{(2)}||\gamma_k^{(2)}| \\
&= \frac{\hat{\kappa}}{2}\|p_k\|_2^2 \frac{\mathcal{O}(\|r_k\|_2\|r_k - q_k\|_2)}{\|q_k\|_2^2} \\
&= \hat{\kappa} \sum_{j=k-m_k}^{k} \mathcal{O}(\|r_j\|_2^2), \qquad (37)
\end{aligned}
$$

where the third equality is due to (34), and the last equality is due to (43) and (44b);

$$\begin{aligned}
\|B_k\|_2 &= \left\| \int_0^1 (g'(x_{k-1} - tp_{k-1}) - g'(x_k - p_k\gamma_k^{(2)} - tp_{k-1}\gamma_k^{(1)}))p_{k-1}\gamma_k^{(1)} dt \right\|_2 \\
&\leq \int_0^1 \|g'(x_{k-1} - tp_{k-1}) - g'(x_k - p_k\gamma_k^{(2)} - tp_{k-1}\gamma_k^{(1)})\|_2 \|p_{k-1}\gamma_k^{(1)}\|_2 dt \\
&\leq \hat{\kappa} \int_0^1 \|\Delta x_{k-1} - p_k\gamma_k^{(2)} - tp_{k-1}\gamma_k^{(1)} + tp_{k-1}\|_2 \|p_{k-1}\|_2 |\gamma_k^{(1)}| dt \\
&\leq \hat{\kappa} \left(\|\Delta x_{k-1}\|_2 + \|p_k\|_2 |\gamma_k^{(2)}| + \frac{1}{2}\|p_{k-1}\|_2 |1 - \gamma_k^{(1)}| \right) \|p_{k-1}\|_2 |\gamma_k^{(1)}| \\
&\leq \hat{\kappa} \left(\|\Delta x_{k-1}\|_2 + \|p_k\|_2 \frac{\|r_k\|_2}{\|q_k\|_2} + \frac{1}{2}\|p_{k-1}\|_2 \frac{\|r_k - q_{k-1}\|_2}{\|q_{k-1}\|_2} \right) \|p_{k-1}\|_2 \frac{\|r_k\|_2}{\|q_{k-1}\|_2} \\
&= \hat{\kappa}\|r_k\|_2 \left(\mathcal{O}(\|\Delta r_{k-1}\|_2) + \mathcal{O}(\|r_k\|_2) + \mathcal{O}(\|r_k - q_{k-1}\|_2) \right. \\
&= \hat{\kappa} \sum_{j=k-m_k}^{k} \mathcal{O}(\|r_j\|_2^2),
\end{aligned} \tag{38}$$

where the last inequality is due to (34), and the second equality is due to (43);

$$\begin{aligned}
\|C_k\|_2 &= \hat{\kappa}\|\Delta r_{\pi(k)-1}\|_2 \sum_{j=k-m_k}^{k-1} \mathcal{O}(\|\Delta r_j\|_2)\gamma_k^{(2)} \\
&\leq \hat{\kappa}\|\Delta r_{\pi(k)-1}\|_2 \frac{\|r_k\|_2}{\|q_k\|_2} \sum_{j=k-m_k}^{k-1} \mathcal{O}(\|\Delta r_j\|_2) \\
&= \hat{\kappa}\|\Delta r_{\pi(k)-1}\|_2 \frac{\|r_k\|_2}{\|q_{\pi(k)}\|_2} \sum_{j=k-m_k}^{k-1} \mathcal{O}(\|\Delta r_j\|_2) \\
&= \hat{\kappa} \sum_{j=k-m_k}^{k} \mathcal{O}(\|r_j\|_2^2),
\end{aligned} \tag{39}$$

where the first inequality is from (34), and the second equality is due to (44b);

$$\begin{aligned}
\|D_k\|_2 &= \hat{\kappa}\|\Delta r_{\upsilon(k)-1}\|_2 \sum_{j=k-m_k}^{k-2} \mathcal{O}(\|\Delta r_j\|_2)\gamma_k^{(1)} \\
&\leq \hat{\kappa}\|\Delta r_{\upsilon(k)-1}\|_2 \frac{\|r_k\|_2}{\|q_{k-1}\|_2} \sum_{j=k-m_k}^{k-2} \mathcal{O}(\|\Delta r_j\|_2) \\
&= \hat{\kappa}\|\Delta r_{\upsilon(k)-1}\|_2 \frac{\|r_k\|_2}{\|q_{\upsilon(k)}\|_2} \sum_{j=k-m_k}^{k-2} \mathcal{O}(\|\Delta r_j\|_2) \\
&= \hat{\kappa} \sum_{j=k-m_k}^{k} \mathcal{O}(\|r_j\|_2^2),
\end{aligned} \tag{40}$$

where the first inequality is from (34), and the second equality is due to (44b). Then with the bounds (37), (38), (39) and (40), we obtain

$$\|H_k\|_2 = \hat{\kappa} \sum_{j=k-m_k}^{k} \|r_j\|_2^2. \tag{41}$$

Combining (31) and (41) to (30), we obtain

$$\|r_{k+1}\| \leq \|\mathcal{L}_k\|_2 + \|\mathcal{H}_k\|_2 \leq \theta_k(\kappa\beta_k + |1 - \beta_k|)\|r_k\|_2 + \hat{\kappa} \sum_{j=k-m_k}^{k} \|r_j\|_2^2,$$

as desired.

□

Remark 4. *There may be some concern about if $\hat{\kappa}$ can be counteracted by the constant hidden in the Big-$\mathcal{O}$ notation. In fact, since $\hat{\kappa}$ is the Lipschitz constant of g' and the constants in $\mathcal{O}(\cdot)$ composes of κ, c_p, c_q, it follows that $\hat{\kappa}$ is unrelated to $\mathcal{O}(\cdot)$. Hence a small $\hat{\kappa}$ can lead to a small uniform boundedness of the higher-order terms. In the extreme case where $\hat{\kappa} = 0$, e.g. g is a linear map, the residual only composes of the first-order term $\mathcal{L}_k$.*

Lemma 1. *Under the same assumptions of Theorem 2, for $k \geq 1$, we have the following bounds:*

$$(1-\kappa)\|\Delta x_{k-1}\|_2 \leq \|\Delta r_{k-1}\|_2 \leq (1+\kappa)\|\Delta x_{k-1}\|_2, \tag{42a}$$

$$(1-\kappa)\|x_k - x^*\|_2 \leq \|r_k\|_2 \leq (1+\kappa)\|x_k - x^*\|_2, \tag{42b}$$

If $q_k \neq 0$, then

$$\frac{\|p_k\|_2}{\|q_k\|_2} \leq \frac{1+c_p}{(1-\kappa)(1-c_q)} \tag{43}$$

If the condition in Line 7 is true, then

$$\|p_k\|_2 \leq (1+c_p)\|\Delta x_{k-1}\|_2, \tag{44a}$$

$$q_k \neq 0,\ (1-c_q)\|\Delta r_{k-1}\| \leq \|q_k\|_2 \leq \|\Delta r_{k-1}\|_2 \tag{44b}$$

Proof. From the assumption (29a) of g, we have

$$\begin{aligned}
(1-\kappa)\|\Delta x_{k-1}\|_2 &\leq \|x_k - x_{k-1}\|_2 - \|g(x_k) - g(x_{k-1})\|_2 \\
&\leq \|g(x_k) - g(x_{k-1}) - (x_k - x_{k-1})\|_2 \\
&= \|r_k - r_{k-1}\|_2 = \|\Delta r_{k-1}\|_2 \\
&\leq \|g(x_k) - g(x_{k-1})\|_2 + \|x_k - x_{k-1}\| \\
&\leq (1+\kappa)\|x_k - x_{k-1}\|_2,
\end{aligned}$$

$$\begin{aligned}
(1-\kappa)\|x_k - x^*\|_2 &\leq \|x_k - x^*\|_2 - \|g(x_k) - g(x^*)\|_2 \\
&\leq \|g(x_k) - g(x^*) - (x_k - x^*)\|_2 = \|r_k\|_2 \\
&\leq \|g(x_k) - g(x^*)\|_2 + \|x_k - x^*\|_2 \\
&\leq (1+\kappa)\|x_k - x^*\|_2.
\end{aligned}$$

If the condition in Line 7 is true, i.e., $\|P_k\zeta_k\|_2 \leq c_p\|\Delta x_{k-1}\|_2, \|Q_k\zeta_k\|_2 \leq c_q\|\Delta r_{k-1}\|_2$, we have

$$\|p_k\|_2 = \|\Delta x_{k-1} - P_k\zeta_k\|_2 \leq \|\Delta x_{k-1}\|_2 + \|P_k\zeta_k\|_2 \leq (1+c_p)\|\Delta x_{k-1}\|_2,$$

$$\|q_k\|_2 = \|\Delta r_{k-1} - Q_k\zeta_k\|_2 \geq \|\Delta r_{k-1}\|_2 - \|Q_k\zeta_k\|_2 \geq (1-c_q)\|\Delta r_{k-1}\|_2.$$

The inequality $\|q_k\|_2 \leq \|\Delta r_{k-1}\|$ is due to the fact that q_k is the orthogonal projection of Δr_{k-1} onto $range(Q_k)^{\perp}$. Also, $q_k \neq 0$ must hold otherwise $q = Q_{k-1}\zeta_k$ which violates the condition $\|Q_k\zeta_k\|_2 < c_q\|\Delta r_{k-1}\|_2$ as $c_q \in (0, 1]$.

If $q_k \neq 0$, then q_k must be updated by Line 8 in some previous iteration. We assume the latest update by Line 8 occurs in the j-th iteration, i.e., $q_k = q_j, p_k = p_j$, hence

$$\frac{\|p_k\|_2}{\|q_k\|_2} = \frac{\|p_j\|_2}{\|q_j\|_2} \leq \frac{(1+c_p)\|\Delta x_{j-1}\|_2}{(1-c_q)\|\Delta r_{j-1}\|_2} \leq \frac{1+c_p}{(1-c_q)(1-\kappa)}.$$

where the first inequality is due to (44a) and (44b) and the second inequality is due to (42a). □

Lemma 2. *Under the same assumptions of Theorem 2, in the k-th iteration ($k \geq 0$) of restart LST-AM (Algorithm 3), we have*

$$p_k + q_k = \int_0^1 g'(x_k - tp_k)p_k dt + \hat{\kappa}\|\Delta r_{\pi(k)-1}\|_2 \sum_{j=k-m_k}^{k-1} \mathcal{O}(\|\Delta r_j\|_2), \tag{45}$$

where $\pi(k)$ denotes that the latest update of q_k by Line 8 occurs in the $\pi(k)$-th iteration and $\pi(k) = k - m_k$ ($m_k = k \mod m$) if Line 8 is never executed up to the k-iteration.

Proof. We prove (45) by induction. Denote $\zeta_k = (\zeta_k^{(1)}, \zeta_k^{(2)})^{\mathrm{T}}$.

For $k = 0$, the relation trivially holds.

For $k = 1$, $p_1 = \Delta x_0, q_1 = \Delta r_0$. It follows that

$$p_1 + q_1 = g(x_1) - g(x_0) = \int_0^1 g'(x_1 - tp_1)p_1 dt.$$

So (45) holds for $k = 1$.

Suppose that (45) holds for $0 \le j \le k-1$, where $k \ge 2$. For $k \ge 2$, if $m_k := k \mod m = 0$ or 1, (45) holds because it is the same as the case of $k = 0$ or $k = 1$. Now consider the nontrivial cases, For $m_k \neq 0$ and $m_k \neq 1$, if the condition in Line 7 in Algorithm 3 is true, Then $\pi(k) = k$. With the convention that $\Delta r_{-1} = 0$, we have

$$\begin{aligned}
p_k + q_k &= \Delta x_{k-1} - P_{k-1}\zeta_k + \Delta r_{k-1} - Q_{k-1}\zeta_k \\
&= g(x_k) - g(x_{k-1}) - (p_{k-1} + q_{k-1})\zeta_k^{(2)} - (p_{k-2} + q_{k-2})\zeta_k^{(1)} \\
&= \int_0^1 g'(x_k - t\Delta x_{k-1})\Delta x_{k-1} dt \\
&\quad - \int_0^1 g'(x_{k-1} - tp_{k-1})p_{k-1}\zeta_k^{(2)} dt + \hat{\kappa}\|\Delta r_{\pi(k-1)-1}\|_2 \sum_{j=k-1-m_{k-1}}^{k-2} \mathcal{O}(\|\Delta r_j\|_2)\zeta_k^{(2)} \\
&\quad - \int_0^1 g'(x_{k-2} - tp_{k-2})p_{k-2}\zeta_k^{(1)} dt + \hat{\kappa}\|\Delta r_{\upsilon(k-1)-1}\|_2 \sum_{j=k-2-m_{k-2}}^{k-3} \mathcal{O}(\|\Delta r_j\|_2)\zeta_k^{(1)}.
\end{aligned} \tag{46}$$

where $\upsilon(k-1) = \pi(\pi(k-1) - 1)$ denotes that q_{k-2} records $q_{\upsilon(k-1)}$ that is the latest update by Line 8 occurred in the $\upsilon(k-1)$-th iteration. Considering the terms in $p_k + q_k$, we know

$$\begin{aligned}
&g'(x_k - t\Delta x_{k-1})\Delta x_{k-1} - g'(x_{k-1} - tp_{k-1})p_{k-1}\zeta_k^{(2)} - g'(x_{k-2} - tp_{k-2})p_{k-2}\zeta_k^{(1)} \\
&= g'(x_k - t\Delta x_{k-1})(\Delta x_{k-1} - p_{k-1}\zeta_k^{(1)} - p_{k-2}\zeta_k^{(1)}) \\
&\quad + (g'(x_k - t\Delta x_{k-1}) - g'(x_{k-1} - tp_{k-1}))p_{k-1}\zeta_k^{(2)} \\
&\quad + (g'(x_k - t\Delta x_{k-1}) - g'(x_{k-2} - tp_{k-2}))p_{k-2}\zeta_k^{(1)}.
\end{aligned} \tag{47}$$

For $\zeta_k = (Q_{k-1}^{\mathrm{T}} Q_{k-1})^{\dagger} Q_{k-1}^{\mathrm{T}} \Delta r_{k-1}$, because $Q_{k-1}^{\mathrm{T}} Q_{k-1} = diag\{\|q_{k-2}\|_2^2, \|q_{k-1}\|_2^2\}$, it follows that

$$\zeta_k^{(1)} = \mathcal{I}(q_{k-2} \neq 0)\frac{\Delta r_{k-1}^{\mathrm{T}} q_{k-2}}{q_{k-2}^{\mathrm{T}} q_{k-2}},\ \zeta_k^{(2)} = \mathcal{I}(q_{k-1} \neq 0)\frac{\Delta r_{k-1}^{\mathrm{T}} q_{k-1}}{q_{k-1}^{\mathrm{T}} q_{k-1}}.$$

Therefore,

$$|\zeta_k^{(1)}| \le \mathcal{I}(q_{k-2} \neq 0)\frac{\|\Delta r_{k-1}\|_2}{\|q_{k-2}\|_2},\ |\zeta_k^{(2)}| \le \mathcal{I}(q_{k-1} \neq 0)\frac{\|\Delta r_{k-1}\|_2}{\|q_{k-1}\|_2}. \tag{48}$$

Now, to bound the terms in (47), we have

$$\begin{aligned}
&\|(g'(x_k - t\Delta x_{k-1}) - g'(x_{k-1} - tp_{k-1}))p_{k-1}\zeta_k^{(2)}\|_2 \\
&\le \hat{\kappa}\|x_k - x_{k-1} - t(\Delta x_{k-1} - p_{k-1})\|_2 \|p_{k-1}\zeta_k^{(2)}\|_2 \\
&\le \hat{\kappa}((1-t)\|\Delta x_{k-1}\|_2 + t\|p_{k-1}\|_2)\|p_{k-1}\|_2 |\zeta_k^{(2)}| \\
&\le \hat{\kappa}((1-t)\|\Delta x_{k-1}\|_2 + t\|p_{k-1}\|_2)\|p_{k-1}\|_2 \mathcal{I}(q_{k-1} \neq 0)\frac{\|\Delta r_{k-1}\|_2}{\|q_{k-1}\|_2} \\
&\le \hat{\kappa}\|\Delta r_{k-1}\|_2 \sum_{j=k-1-m_{k-1}}^{k-1} \mathcal{O}(\|\Delta r_j\|_2) = \hat{\kappa}\|\Delta r_{k-1}\|_2 \sum_{j=k-m_k}^{k-1} \mathcal{O}(\|\Delta r_j\|_2),
\end{aligned} \tag{49}$$

where the third inequality is due to (48), and the last inequality is due to (42a), (44a) and (43), where the constants are absorbed into the big-$\mathcal{O}$ notation. Similarly, it follows that

$$\begin{aligned}
&\|(g'(x_k - t\Delta x_{k-1}) - g'(x_{k-2} - tp_{k-2}))p_{k-2}\zeta_k^{(1)}\|_2 \\
&\leq \hat{\kappa}\|\Delta x_{k-1} + \Delta x_{k-2} - t\Delta x_{k-1} + tp_{k-2}\|_2\|p_{k-2}\zeta_k^{(1)}\|_2 \\
&\leq \hat{\kappa}((1-t)\|\Delta x_{k-1}\|_2 + \|\Delta x_{k-2}\|_2 + t\|p_{k-2}\|_2)\|p_{k-2}\|_2|\zeta_k^{(1)}| \\
&\leq \hat{\kappa}((1-t)\|\Delta x_{k-1}\|_2 + \|\Delta x_{k-2}\|_2 + t\|p_{k-2}\|_2)\|p_{k-2}\|_2\mathcal{I}(q_{k-2} \neq 0)\frac{\|\Delta r_{k-1}\|_2}{\|q_{k-2}\|_2} \\
&\leq \hat{\kappa}\|\Delta r_{k-1}\|_2 \sum_{j=k-2-m_{k-2}}^{k-1} \mathcal{O}(\|\Delta r_j\|_2) = \hat{\kappa}\|\Delta r_{k-1}\|_2 \sum_{j=k-m_k}^{k-1} \mathcal{O}(\|\Delta r_j\|_2). \qquad (50)
\end{aligned}$$

For the remaining terms in (46), we have

$$\begin{aligned}
&\hat{\kappa}\|\Delta r_{\pi(k-1)-1}\|_2 \sum_{j=k-1-m_{k-1}}^{k-2} \mathcal{O}(\|\Delta r_j\|_2)\zeta_k^{(2)} + \hat{\kappa}\|\Delta r_{\upsilon(k-1)-1}\|_2 \sum_{k=k-2-m_{k-2}}^{k-3} \mathcal{O}(\|\Delta r_j\|_2)\zeta_k^{(1)} \\
&\leq \hat{\kappa}\|\Delta r_{\pi(k-1)-1}\|_2\mathcal{I}(q_{k-1} \neq 0)\frac{\|\Delta r_{k-1}\|_2}{\|q_{k-1}\|_2} \sum_{j=k-1-m_{k-1}}^{k-2} \mathcal{O}(\|\Delta r_j\|_2) \\
&\quad + \hat{\kappa}\|\Delta r_{\upsilon(k-1)-1}\|_2\mathcal{I}(q_{k-2} \neq 0)\frac{\|\Delta r_{k-1}\|_2}{\|q_{k-2}\|_2} \sum_{k=k-2-m_{k-2}}^{k-3} \mathcal{O}(\|\Delta r_j\|_2) \\
&\leq \hat{\kappa}\|\Delta r_{k-1}\|_2 \sum_{k=k-m_k}^{k-2} \mathcal{O}(\|\Delta r_j\|_2), \qquad (51)
\end{aligned}$$

where the last inequality is due to (44b) and that $q_{k-1} = q_{\pi(k-1)}, q_{k-2} = q_{\upsilon(k-1)}$.

With relations (46), (47), (49), (50) and (51), and noting that $p_k = \Delta x_{k-1} - p_{k-1}\zeta_k^{(2)} - p_{k-2}\zeta_k^{(1)}$, and

$$\begin{aligned}
&\left\|\int_0^1 (g'(x_k - t\Delta x_{k-1})\Delta x_{k-1} - g'(x_{k-1} - tp_{k-1})p_{k-1}\zeta_k^{(2)} - g'(x_{k-2} - tp_{k-2})p_{k-2}\zeta_k^{(1)})dt\right\|_2 \\
&\leq \int_0^0 \|g'(x_k - t\Delta x_{k-1})\Delta x_{k-1} - g'(x_{k-1} - tp_{k-1})p_{k-1}\zeta_k^{(2)} - g'(x_{k-2} - tp_{k-2})p_{k-2}\zeta_k^{(1)}\|_2 dt,
\end{aligned}$$

we can estimate $p_k + q_k$ as

$$p_k + q_k = \int_0^1 g'(x_k - t\Delta x_{k-1})p_k dt + \hat{\kappa}\|\Delta r_{k-1}\|_2 \sum_{j=k-m_k}^{k-1} \mathcal{O}(\|\Delta r_j\|_2). \qquad (52)$$

To further obtain (45), notice that the difference

$$\begin{aligned}
&\left\|\int_0^1 g'(x_k - tp_k)p_k dt - \int_0^1 g'(x_k - t\Delta x_{k-1})p_k dt\right\|_2 \\
&= \left\|\int_0^1 (g'(x_k - tp_k) - g'(x_k - t\Delta x_{k-1}))p_k dt\right\|_2 \\
&\leq \int_0^1 \|g'(x_k - tp_k) - g'(x_k - t\Delta x_{k-1})\|_2\|p_k\|_2 dt \\
&\leq \hat{\kappa}\int_0^1 t\|p_{k-1}\zeta_k^{(2)} + p_{k-2}\zeta_k^{(1)}\|_2\|p_k\|_2 dt \\
&\leq \frac{\hat{\kappa}}{2}c_p\|\Delta x_{k-1}\|_2\|p_k\|_2 = \mathcal{O}\|\Delta r_{k-1}\|_2^2,
\end{aligned}$$

where the last inequality is due to the condition $\|P_{k-1}\zeta_k\|_2 < c_p\|p\|_2$ and inequalities (42a) and (44a). Hence the difference can be absorbed in the Big-$\mathcal{O}$ notation in (52). Thus (45) holds when the condition in Line 7 is true for the k-th iteration.

We consider the case where the condition in Line 7 is false for the k-th iteration. Then $P_k = P_{k-1}, Q_k = Q_{k-1}$. In other words, the memory recording p_k, q_k keeps unchanged from the $(\pi(k)+1)$-th to k-th iteration. Since $\pi(k) < k$ and $\pi(\pi(k)) = \pi(k)$, with the inductive hypothesis, we have

$$\begin{aligned} p_k + q_k &= p_{\pi(k)} + q_{\pi(k)} \\ &= \int_0^1 g'(x_{\pi(k)} - tp_{\pi(k)})p_{\pi(k)}dt + \hat{\kappa}\|\Delta r_{\pi(k)-1}\|_2 \sum_{j=\pi(k)-m_{\pi(k)}}^{\pi(k)-1} \mathcal{O}(\|\Delta r_j\|_2) \\ &= \int_0^1 g'(x_{\pi(k)} - tp_k)p_k dt + \hat{\kappa}\|\Delta r_{\pi(k)-1}\| \sum_{j=k-m_k}^{k-1} \mathcal{O}(\|\Delta r_j\|_2). \end{aligned} \tag{53}$$

To further obtain (45), note that the difference

$$\begin{aligned} &\left\| \int_0^1 g'(x_k - tp_k)p_k dt - \int_0^1 g'(x_{\pi(k)} - tp_k)p_k dt \right\|_2 \\ &\le \int_0^1 \|g'(x_k - tp_k) - g'(x_{\pi(k)} - tp_k)\|_2 \|p_k\|_2 dt \\ &\le \hat{\kappa}\|x_k - x_{\pi(k)}\|_2\|p_k\|_2 \\ &= \hat{\kappa} \sum_{j=\pi(k)}^{k-1} \|\Delta x_j\|_2\|p_k\|_2 = \hat{\kappa}\|\Delta r_{\pi(k)-1}\|_2 \sum_{j=\pi(k)}^{k-1} \mathcal{O}(\|\Delta r_j\|_2) \end{aligned}$$

can be absorbed into the Big-$\mathcal{O}$ notation in (53). Thus (45) also holds when the condition in Line 7 is false for the k-th iteration.

As a result, we complete the induction in the k-th iteration. □

A.3 Regularized short-term recurrence Anderson mixing

A.3.1 Check of positive definiteness

We describe the check of positive definiteness in RST-AM, which follows the same procedure of that of SAM (Wei et al., 2021). From Line 11-13 in Algorithm 1, one update of x_k RST-AM is $x_{k+1} = x_k + H_k r_k$, where $H_k = \beta_k I - \alpha_k Y_k Z_k^\dagger Q_k^{\mathrm{T}}$, $Y_k = P_k + \beta_k Q_k$, $Z_k = Q_k^{\mathrm{T}} Q_k + \delta_k P_k^{\mathrm{T}} P_k$. H_k is generally not symmetric. A critical condition for the convergence analysis of RST-AM is the *positive definiteness* of H_k, i.e.

$$s_k^{\mathrm{T}} H_k s_k \ge \beta_k \mu \|s_k\|_2^2, \quad \forall s_k \in \mathbb{R}^d, \tag{54}$$

where $\mu \in (0, 1)$ is a constant. Next, we give an approach to guarantee it.

Let $\lambda_{min}(\cdot)$ denote the smallest eigenvalue, $\lambda_{max}(\cdot)$ denote the largest eigenvalue. Since $s_k^{\mathrm{T}} H_k s_k = \frac{1}{2} s_k^{\mathrm{T}}(H_k + H_k^{\mathrm{T}})s_k$, Condition (54) is equivalent to $\lambda_{min}\left(\frac{1}{2}\left(H_k + H_k^{\mathrm{T}}\right)\right) \ge \beta_k \mu$. With some simple algebraic operations, we obtain $\lambda_{min}\left(\frac{1}{2}\left(H_k + H_k^{\mathrm{T}}\right)\right) = \beta_k - \frac{1}{2}\alpha_k \lambda_{max}(Y_k Z_k^\dagger Q_k^{\mathrm{T}} + Q_k Z_k^\dagger Y_k^{\mathrm{T}})$. Let $\lambda_k \stackrel{\text{def}}{=} \lambda_{max}(Y_k Z_k^\dagger Q_k^{\mathrm{T}} + Q_k Z_k^\dagger Y_k^{\mathrm{T}})$, then Condition (54) is equivalent to

$$\alpha_k \lambda_k \le 2\beta_k(1 - \mu), \tag{55}$$

namely, (13) in Remark 3. To check Condition (55), note that

$$\lambda_k = \lambda_{max}\left(\begin{pmatrix} Y_k & Q_k \end{pmatrix} \begin{pmatrix} 0 & Z_k^\dagger \\ Z_k^\dagger & 0 \end{pmatrix} \begin{pmatrix} Y_k^{\mathrm{T}} \\ Q_k^{\mathrm{T}} \end{pmatrix} \right) = \lambda_{max}\left(\begin{pmatrix} Y_k^{\mathrm{T}} \\ Q_k^{\mathrm{T}} \end{pmatrix} \begin{pmatrix} Y_k & Q_k \end{pmatrix} \begin{pmatrix} 0 & Z_k^\dagger \\ Z_k^\dagger & 0 \end{pmatrix} \right). \tag{56}$$

Since $\begin{pmatrix} Y_k^{\mathrm{T}} \\ Q_k^{\mathrm{T}} \end{pmatrix} \begin{pmatrix} Y_k & Q_k \end{pmatrix}, \begin{pmatrix} 0 & Z_k^\dagger \\ Z_k^\dagger & 0 \end{pmatrix} \in \mathbb{R}^{4\times 4}$, λ_k can be computed cheaply. This cost is negligible compared with those to form $P_k^{\mathrm{T}} P_k, Q_k^{\mathrm{T}} Q_k$, which need $O(d)$ flops. After that, to guarantee the positive definiteness, we check if α_k satisfies (55) and use a smaller α_k if necessary, e.g. $\alpha_k = \max\{2\beta_k(1 - \mu)/\lambda_k, 0\}$.

A.3.2 PROOFS OF THE THEOREMS

We first give the proof of the boundedness of $\|P_{k-1}\zeta_k\|_2$ and $\|Q_{k-1}\zeta_k\|_2$.

Lemma 3. *For $P, Q \in \mathbb{R}^{d\times m}(d \geq m), \delta > 0$, and $Z = Q^{\mathrm{T}}Q + \delta P^{\mathrm{T}}P$, we have*

$$\|PZ^{\dagger}Q^{\mathrm{T}}\|_2 \leq \delta^{-\frac{1}{2}}, \tag{57a}$$

$$\|QZ^{\dagger}Q^{\mathrm{T}}\|_2 \leq 1. \tag{57b}$$

Proof. We first consider the case that Z is nonsingular, then $PZ^{\dagger}Q^{\mathrm{T}} = PZ^{-1}Q^{\mathrm{T}}, QZ^{\dagger}Q^{\mathrm{T}} = QZ^{-1}Q^{\mathrm{T}}$. It can be seen that $P^{\mathrm{T}}P$ and $Q^{\mathrm{T}}Q$ are symmetric positive semidefinite, and Z is SPD as it is assumed to be nonsingular. Also, we have $\delta P^{\mathrm{T}}P \preceq Z$ and $Q^{\mathrm{T}}Q \preceq Z$, where the notation "$\preceq$" denotes the *Loewner partial order*, i.e., $A \preceq B$ with $A, B \in \mathbb{R}^{m\times m}$ means that $B - A$ is positive semidefinite. Hence, we have

$$Z^{-\frac{1}{2}}\delta P^{\mathrm{T}}PZ^{-\frac{1}{2}} \preceq I, Z^{-\frac{1}{2}}Q^{\mathrm{T}}QZ^{-\frac{1}{2}} \preceq I,$$

which implies

$$\|Z^{-\frac{1}{2}}\left(P^{\mathrm{T}}P\right)Z^{-\frac{1}{2}}\|_2 \leq \delta^{-1},$$
$$\|Z^{-\frac{1}{2}}\left(Q^{\mathrm{T}}Q\right)Z^{-\frac{1}{2}}\|_2 \leq 1.$$

Let $\lambda_max(\cdot)$ denote the largest eigenvalue, we have

$$\|QZ^{-1}Q^{\mathrm{T}}\|_2 = \lambda_{max}\left(QZ^{-1}Q^{\mathrm{T}}\right) = \lambda_{max}\left(Q^{\mathrm{T}}QZ^{-1}\right) = \lambda_{max}\left(Z^{-\frac{1}{2}}Q^{\mathrm{T}}QZ^{-\frac{1}{2}}\right) \leq 1,$$

$$\begin{aligned}
\|PZ^{-1}Q^{\mathrm{T}}\|_2^2 &= \lambda_{max}\left(PZ^{-1}Q^{\mathrm{T}}QZ^{-1}P^{\mathrm{T}}\right)\\
&= \lambda_{max}\left(P^{\mathrm{T}}PZ^{-1}Q^{\mathrm{T}}QZ^{-1}\right)\\
&= \lambda_{max}\left(Z^{-\frac{1}{2}}\left(P^{\mathrm{T}}P\right)Z^{-\frac{1}{2}}\cdot Z^{-\frac{1}{2}}\left(Q^{\mathrm{T}}Q\right)Z^{-\frac{1}{2}}\right)\\
&\leq \|Z^{-\frac{1}{2}}\left(P^{\mathrm{T}}P\right)Z^{-\frac{1}{2}}\cdot Z^{-\frac{1}{2}}\left(Q^{\mathrm{T}}Q\right)Z^{-\frac{1}{2}}\|_2\\
&\leq \|Z^{-\frac{1}{2}}\left(P^{\mathrm{T}}P\right)Z^{-\frac{1}{2}}\|_2\|Z^{-\frac{1}{2}}\left(Q^{\mathrm{T}}Q\right)Z^{-\frac{1}{2}}\|_2 \leq \delta^{-1}.
\end{aligned}$$

Therefore, $\|PZ^{-1}Q^{\mathrm{T}}\| \leq \delta^{-\frac{1}{2}}$ and $\|QZ^{-1}Q^{\mathrm{T}}\|_2 \leq 1$.

For the case that Z is singular, it can be proved that

$$ker(Z) := \{x \in \mathbb{R}^m | Zx = 0\} = \{x \in \mathbb{R}^m | Px = 0 \text{ and } Qx = 0\}. \tag{58}$$

In fact, if $Px = 0$ and $Qx = 0$, it is obvious that $Zx = 0$. In the other side, if $Zx = 0$, then $x^{\mathrm{T}}Zx = 0$, i.e. $x^{\mathrm{T}}Q^{\mathrm{T}}Qx + \delta x^{\mathrm{T}}P^{\mathrm{T}}Px = 0$. Since $0 \preceq P^{\mathrm{T}}P, 0 \preceq Q^{\mathrm{T}}Q, \delta > 0$, it follows that $x^{\mathrm{T}}Q^{\mathrm{T}}Qx = 0$ and $\delta x^{\mathrm{T}}P^{\mathrm{T}}Px = 0$, which further implies $Qx = 0$ and $Px = 0$. Hence (58) holds.

Let U_1 satisfy $U_1^{\mathrm{T}}U_1 = I$ and $range(U_1) = ker(Z)$, i.e. the orthonormal basis of $ker(Z)$, and U_2 satisfy $U_2^{\mathrm{T}}U_2 = I$ and $U_2^{\mathrm{T}}U_1 = 0$, i.e. the orthonormal basis of $ker(Z)^{\perp}$. With the equality (58), we know $PU_1 = 0, QU_1 = 0$. Define $U = (U_1, U_2) \in \mathbb{R}^{m\times m}$, then $U^{\mathrm{T}}U = I_m$ and by direct computation, we have

$$U^{\mathrm{T}}ZU = \begin{pmatrix} 0 & 0 \\ 0 & U_2^{\mathrm{T}}ZU_2 \end{pmatrix},$$

where $U_2^{\mathrm{T}}ZU_2 = (QU_2)^{\mathrm{T}}QU_2 + \delta(PU_2)^{\mathrm{T}}PU_2$ is nonsingular according to the definition of U_2. So

$$Z^{\dagger} = U\begin{pmatrix} 0 & 0 \\ 0 & (U_2^{\mathrm{T}}ZU_2)^{-1} \end{pmatrix}U^{\mathrm{T}}.$$

As a result, we can further compute $PZ^{\dagger}Q^{\mathrm{T}}$ and $QZ^{\dagger}Q^{\mathrm{T}}$ as

$$PZ^{\dagger}Q^{\mathrm{T}} = (PU_2)(U_2^{\mathrm{T}}ZU_2)^{-1}(QU_2)^{\mathrm{T}},\ QZ^{\dagger}Q^{\mathrm{T}} = (QU_2)(U_2^{\mathrm{T}}ZU_2)^{-1}(QU_2)^{\mathrm{T}}.$$

Then let $\hat{P} = PU_2, \hat{Q} = QU_2$, and $\hat{Z} = \hat{Q}^{\mathrm{T}}\hat{Q} + \delta\hat{P}^{\mathrm{T}}\hat{P}$, and noting that $\hat{Z}$ is nonsingular, we can obtain $\|PZ^{\dagger}Q^{\mathrm{T}}\|_2 = \|\hat{P}\hat{Z}^{-1}\hat{Q}^{\mathrm{T}}\|_2 \leq \delta^{-\frac{1}{2}}$, $\|QZ^{\dagger}Q^{\mathrm{T}}\|_2 = \|\hat{Q}\hat{Z}^{-1}\hat{Q}^{\mathrm{T}}\|_2 \leq 1$. □

As a result of Lemma 3, $\|P_{k-1}\zeta_k\|_2, \|Q_{k-1}\zeta_k\|_2$ in Algorithm 1 are bounded by $\mathcal{O}(\|\Delta r_{k-1}\|_2)$, as shown in the following corollary.

Corollary 2. *$\|P_{k-1}\zeta_k\|_2, \|Q_{k-1}\zeta\|_2$ in Algorithm 1 are bounded, i.e.*

$$\|P_{k-1}\zeta_k\|_2 \leq (\delta_k^{(1)})^{-\frac{1}{2}}\|\Delta r_{k-1}\|_2,\ \|Q_{k-1}\zeta_k\|_2 \leq \|\Delta r_{k-1}\|_2, \tag{59}$$

where $\zeta_k = (Q_{k-1}^{\mathrm{T}}Q_{k-1} + \delta_k^{(1)}P_{k-1}P_{k-1})^{\dagger}Q_{k-1}^{\mathrm{T}}\Delta r_{k-1}$.

Now, we turn to the proofs the theorems about RST-AM in Section 3.4. For brevity, we use δ_k to denote $\delta_k^{(2)}$, i.e. $\delta_k \equiv \delta_k^{(2)}$.

From Assumption 2, for the mini-batch gradient $f_{S_k}(x_k) = \frac{1}{n_k}\sum_{i\in S_k} f_{\xi_i}(x_k)$, where $n_k = |S_k|$, we have

$$\mathbb{E}[\nabla f_{S_k}(x)|x_k] = \nabla f(x_k), \tag{60a}$$

$$\mathbb{E}[\|\nabla f_{S_k}(x_k) - \nabla f(x_k)\|_2^2|x_k] \leq \frac{\sigma^2}{n_k}. \tag{60b}$$

Note that the update of RST-AM (Line 11-13 in Algorithm 1) can be written as $x_{k+1} = x_k + H_k r_k$, where $r_k = -\nabla f_{S_k}(x_k)$, and for $k \geq 0$,

$$H_k = \beta_k I - \alpha_k\left(P_k + \beta_k Q_k\right)\left(Q_k^{\mathrm{T}}Q_k + \delta_k P_k^{\mathrm{T}}P_k\right)^{\dagger}Q_k^{\mathrm{T}}. \tag{61}$$

To prove the theorems, the critical points are (i) the positive definiteness of the approximate Hessian H_k and (ii) an adequate suppression of the noise in the gradient estimation for the stochastic case.

We first give a lemma related to the projection step.

Lemma 4. *Suppose that $\{x_k\}$ is generated by RST-AM. If $\alpha_k \geq 0, \beta_k > 0, \delta_k > 0$, then for any $v_k \in \mathbb{R}^d$, we have*

$$\|H_k v_k\|_2^2 \leq 2\left(\beta_k^2\left(1 + 2\alpha_k^2 - 2\alpha_k\right) + \alpha_k^2\delta_k^{-1}\right)\|v_k\|_2^2. \tag{62}$$

Proof. The result clearly holds when $k = 0$ as $H_0 = \beta_0 I$. For $k \geq 1$,

$$H_k v_k = \beta_k v_k - (\alpha_k P_k + \alpha_k\beta_k Q_k)\Gamma_k, \tag{63}$$

where

$$\Gamma_k = \min_{\Gamma}\|v_k - Q_k\Gamma\|_2^2 + \delta_k\|P_k\Gamma\|_2^2. \tag{64}$$

Taking $\Gamma = 0$, we have

$$\|v_k - Q_k\Gamma_k\|_2^2 + \delta_k\|P_k\Gamma_k\|_2^2 \leq \|v_k\|_2^2. \tag{65}$$

Therefore,

$$\begin{aligned}
&\|H_k v_k\|_2^2 \\
&= \|\beta_k v_k - (\alpha_k P_k + \alpha_k\beta_k Q_k)\Gamma_k\|_2^2 \\
&= \|\beta_k\left(v_k - \alpha_k Q_k\Gamma_k\right) - \alpha_k P_k\Gamma_k\|_2^2 \\
&= \|\beta_k(1-\alpha_k)v_k + \beta_k\alpha_k(v_k - Q_k\Gamma_k) - \alpha_k\delta_k^{-\frac{1}{2}}\delta_k^{\frac{1}{2}}P_k\Gamma_k\|_2^2 \\
&\leq \left(\beta_k^2(1-\alpha_k)^2 + \beta_k^2\alpha_k^2 + \alpha_k^2\delta_k^{-1}\right)\cdot\left(\|v_k\|_2^2 + \|v_k - Q_k\Gamma_k\|_2^2 + \delta_k\|P_k\Gamma_k\|_2^2\right) \\
&\leq \left(\beta_k^2\left(1 + 2\alpha_k^2 - 2\alpha_k\right) + \alpha_k^2\delta_k^{-1}\right)\left(\|v_k\|_2^2 + \|v_k\|_2^2\right) \\
&= 2\left(\beta_k^2\left(1 + 2\alpha_k^2 - 2\alpha_k\right) + \alpha_k^2\delta_k^{-1}\right)\|v_k\|_2^2.
\end{aligned} \tag{66}$$

In the above, the first inequality uses the inequality

$$\|\sum_{i=1}^{n} a_i\mathbf{x_i}\|_2^2 \leq \left(\sum_{i=1}^{n}|a_i|\|\mathbf{x_i}\|_2\right)^2 \leq \left(\sum_{i=1}^{n}a_i^2\right)\left(\sum_{i=1}^{n}\|\mathbf{x_i}\|_2^2\right), \tag{67}$$

where $a_i \in \mathbb{R}, x_i \in \mathbb{R}^d$. The second inequality is based on inequality (65). □

With Lemma 4, we can prove the deterministic case of RST-AM.

Proof of Theorem 3. Since $1+2\alpha_k^2-2\alpha_k \leq 1$ for $0 \leq \alpha_k \leq 1$, and $\delta_k^{-1} \leq C^{-1}\beta^2$, with Lemma 4, we have

$$\|H_k r_k\|_2^2 \leq 2\beta^2(1+C^{-1})\|r_k\|_2^2.$$

Since α_k satisfies (55), we have

$$r_k^{\mathrm{T}} H_k r_k \geq \beta\mu\|r_k\|_2^2.$$

Then, under Assumption 1, we have

$$\begin{aligned} f(x_{k+1}) &\leq f(x_k) + \nabla f(x_k)^{\mathrm{T}}(x_{k+1}-x_k) + \frac{L}{2}\|x_{k+1}-x_k\|_2^2 \\ &= f(x_k) - r_k^{\mathrm{T}} H_k r_k + \frac{L}{2}\|H_k r_k\|_2^2 \\ &\leq f(x_k) - \beta\mu\|r_k\|_2^2 + L\beta^2(1+C^{-1})\|r_k\|_2^2 \\ &= f(x_k) - \beta\left(\mu - \beta L(1+C^{-1})\right)\|r_k\|_2^2 \\ &\leq f(x_k) - \frac{1}{2}\beta\mu \cdot \|\nabla f(x_k)\|_2^2, \end{aligned} \tag{68}$$

where the last inequality is due to $0 < \beta \leq \frac{\mu}{2L(1+C^{-1})}$. Thus, $f(x_{k+1}) - f(x_k) \leq -\frac{1}{2}\beta\mu\|\nabla f(x_k)\|_2^2$.

Summing both sides of this inequality for $k \in \{0,\ldots,N-1\}$ and recalling $f(x) > f^{low}$ in Assumption 1 gives

$$f^{low} - f(x_0) \leq f(x_N) - f(x_0) \leq -\frac{1}{2}\beta\mu\sum_{k=0}^{N-1}\|\nabla f(x_k)\|_2^2.$$

Rearranging and dividing further by N yields (15). □

The next lemmas and proofs are about the stochastic case.

Lemma 5. *Suppose that Assumption 2 holds for $\{x_k\}$ generated by RST-AM. In addition, if $\beta_k > 0, \delta_k > 0$, and $\alpha_k \geq 0$ and satisfies (13), then*

$$\mathbb{E}_{S_k}[\|H_k r_k\|_2^2] \leq 2\left(\beta_k^2\left(1+2\alpha_k^2-2\alpha_k\right) + \frac{\alpha_k^2}{\delta_k}\right)\cdot\left(\|\nabla f(x_k)\|_2^2 + \frac{\sigma^2}{n_k}\right), \tag{69a}$$

$$\nabla f(x_k)^{\mathrm{T}}\mathbb{E}_{S_k}[H_k r_k] \leq -\frac{1}{2}\beta_k\mu\|\nabla f(x_k)\|_2^2 + \frac{1}{2}\frac{\alpha_k^2(\delta_k^{-\frac{1}{2}}+\beta_k)^2}{\beta_k\mu}\cdot\frac{\sigma^2}{n_k}, \tag{69b}$$

where $\mu > 0$ is the constant introduced in Note 3.

Proof. (i) From Lemma 4, we have

$$\mathbb{E}_{S_k}[\|H_k r_k\|_2^2] \leq 2\left(\beta_k^2\left(1+2\alpha_k^2-2\alpha_k\right) + \frac{\alpha_k^2}{\delta_k}\right)\mathbb{E}_{S_k}[\|r_k\|_2^2]. \tag{70}$$

From Assumption 2, we have

$$\mathbb{E}_{S_k}[\|r_k\|_2^2] = \mathbb{E}_{S_k}[\|r_k - \mathbb{E}_{S_k}[r_k]\|_2^2] + \|\mathbb{E}_{S_k}[r_k]\|_2^2 = \|\nabla f(x_k)\|_2^2 + \sigma^2/n_k. \tag{71}$$

With (70), (71), we obtain (69a).

(ii) Recalling that $H_0 = \beta_0 I$, the result holds for $k=0$. Define $\epsilon_k = \nabla f_{S_k}(x_k) - \nabla f(x_k) = -r_k - \nabla f(x_k)$, then $H_k r_k = H_k\left(-\epsilon_k - \nabla f(x_k)\right)$. Since α_k satisfies (13), we can ensure $\lambda_{min}\left(\frac{1}{2}\left(H_k + H_k^{\mathrm{T}}\right)\right) \geq \beta_k\mu$. Thus

$$\nabla f(x_k)^{\mathrm{T}} H_k \nabla f(x_k) = \frac{1}{2}\nabla f(x_k)^{\mathrm{T}}\left(H_k + H_k^{\mathrm{T}}\right)\nabla f(x_k) \geq \beta_k\mu\|\nabla f(x_k)\|_2^2,$$

which implies

$$\mathbb{E}_{S_k}[\nabla f(x_k)^{\mathrm{T}} H_k \nabla f(x_k)] \geq \beta_k\mu\|\nabla f(x_k)\|_2^2. \tag{72}$$

Let $M_k = \alpha_k \left(P_k + \beta_k Q_k\right) \left(Q_k^{\mathrm{T}} Q_k + \delta_k P_k^{\mathrm{T}} P_k\right)^{\dagger} Q_k^{\mathrm{T}}$, then $H_k = \beta_k I - M_k$. With the assumption (60a), i.e. $\mathbb{E}_{S_k}[\epsilon_k] = 0$, we have

$$\begin{aligned}\mathbb{E}_{S_k}[\nabla f(x_k)^{\mathrm{T}} H_k \epsilon_k] &= \mathbb{E}_{S_k}[\nabla f(x_k)^{\mathrm{T}} \left(\beta_k \epsilon_k - M_k \epsilon_k\right)] \\ &= \beta_k \nabla f(x_k)^{\mathrm{T}} \mathbb{E}_{S_k}[\epsilon_k] - \mathbb{E}_{S_k}[\nabla f(x_k)^{\mathrm{T}} M_k \epsilon_k] = -\mathbb{E}_{S_k}[\nabla f(x_k)^{\mathrm{T}} M_k \epsilon_k].\end{aligned}$$

Using the *Cauchy-Schwarz inequality with expectations*, we obtain

$$\begin{aligned}|\mathbb{E}_{S_k}[\nabla f(x_k)^{\mathrm{T}} H_k \epsilon_k]| = |\mathbb{E}_{S_k}[\nabla f(x_k)^{\mathrm{T}} M_k \epsilon_k]| &\leq \sqrt{\mathbb{E}_{S_k}[\|\nabla f(x_k)\|_2^2]} \sqrt{\mathbb{E}_{S_k}[\|M_k \epsilon_k\|_2^2]} \\ &\leq \|\nabla f(x_k)\|_2 \sqrt{\mathbb{E}_{S_k}[\|M_k \epsilon_k\|_2^2]}. \end{aligned} \tag{73}$$

We now bound $\|M_k \epsilon_k\|_2^2$. For brevity, let $Z_k = Q_k^{\mathrm{T}} Q_k + \delta_k P_k^{\mathrm{T}} P_k$, and $N_1 = P_k Z_k^{\dagger} Q_k^{\mathrm{T}}, N_2 = \beta_k Q_k Z_k^{\dagger} Q_k^{\mathrm{T}}$, then

$$\|M_k\|_2 = \|\alpha_k \left(N_1 + N_2\right)\|_2 \leq \alpha_k \left(\|N_1\|_2 + \|N_2\|_2\right) \leq \alpha_k (\delta_k^{-\frac{1}{2}} + \beta_k), \tag{74}$$

where the last inequality is from Lemma 3.

With (74), we have $\|M_k \epsilon_k\|_2 \leq \alpha_k (\delta_k^{-\frac{1}{2}} + \beta_k) \|\epsilon_k\|_2$, which implies

$$\mathbb{E}_{S_k}[\|M_k \epsilon_k\|_2^2] \leq \alpha_k^2 (\delta_k^{-\frac{1}{2}} + \beta_k)^2 \mathbb{E}_{S_k}[\|\epsilon_k\|_2^2] \leq \alpha_k^2 (\delta_k^{-\frac{1}{2}} + \beta_k)^2 \frac{\sigma^2}{n_k}, \tag{75}$$

where the last inequality is due to (60b). Now we can obtain the bound of $|\mathbb{E}_{S_k}[\nabla f(x_k)^{\mathrm{T}} H_k \epsilon_k]|$ as follows (cf. (73)):

$$\begin{aligned}&|\mathbb{E}_{S_k}[\nabla f(x_k)^{\mathrm{T}} H_k \epsilon_k]| \\ &\leq \|\nabla f(x_k)\|_2 \sqrt{\mathbb{E}_{S_k}[\|M_k \epsilon_k\|_2^2]} \\ &\leq \alpha_k (\delta_k^{-\frac{1}{2}} + \beta_k) \|\nabla f(x_k)\|_2 \sqrt{\mathbb{E}_{S_k}[\|\epsilon_k\|_2^2]} \\ &\leq \alpha_k (\delta_k^{-\frac{1}{2}} + \beta_k) \frac{\sigma}{\sqrt{n_k}} \|\nabla f(x_k)\|_2 \\ &= \sqrt{\beta_k \mu} \|\nabla f(x_k)\|_2 \cdot \frac{\alpha_k (\delta_k^{-\frac{1}{2}} + \beta_k)}{\sqrt{\beta_k \mu}} \frac{\sigma}{\sqrt{n_k}} \\ &\leq \frac{1}{2} \beta_k \mu \|\nabla f(x_k)\|_2^2 + \frac{1}{2} \frac{\alpha_k^2 (\delta_k^{-\frac{1}{2}} + \beta_k)^2}{\beta_k \mu} \cdot \frac{\sigma^2}{n_k}.\end{aligned} \tag{76}$$

With the inequality (72) and (76), we obtain

$$\begin{aligned}&\nabla f(x_k)^{\mathrm{T}} \mathbb{E}_{S_k}[H_k r_k] \\ &= -\nabla f(x_k)^{\mathrm{T}} \mathbb{E}_{S_k}[H_k \left(\epsilon_k + \nabla f(x_k)\right)] \\ &= -\mathbb{E}_{S_k}[\nabla f(x_k)^{\mathrm{T}} H_k \nabla f(x_k)] - \mathbb{E}_{S_k}[\nabla f(x_k)^{\mathrm{T}} H_k \epsilon_k] \\ &\leq -\mathbb{E}_{S_k}[\nabla f(x_k)^{\mathrm{T}} H_k \nabla f(x_k)] + |\mathbb{E}_{S_k}[\nabla f(x_k)^{\mathrm{T}} H_k \epsilon_k]| \\ &\leq -\beta_k \mu \|\nabla f(x_k)\|_2^2 + \frac{1}{2} \beta_k \mu \|\nabla f(x_k)\|_2^2 + \frac{1}{2} \frac{\alpha_k^2 (\delta_k^{-\frac{1}{2}} + \beta_k)^2}{\beta_k \mu} \cdot \frac{\sigma^2}{n_k} \\ &= -\frac{1}{2} \beta_k \mu \|\nabla f(x_k)\|_2^2 + \frac{1}{2} \frac{\alpha_k^2 (\delta_k^{-\frac{1}{2}} + \beta_k)^2}{\beta_k \mu} \cdot \frac{\sigma^2}{n_k}.\end{aligned} \tag{77}$$

□

By imposing more restrictions to $\alpha_k, \beta_k, \delta_k$, we can obtain a convenient corollary:

Corollary 3. *Suppose that Assumption 2 holds for $\{x_k\}$ generated by RST-AM. $C > 0$ is the constant in (12). If $\beta_k > 0, \delta_k \geq C\beta_k^{-2}$, $0 \leq \alpha_k \leq \min\{1, \beta_k^{\frac{1}{2}}\}$ and satisfies (55) , then*

$$\mathbb{E}_{S_k}[\|H_k r_k\|_2^2] \leq 2\beta_k^2 \left(1 + C^{-1}\right) \cdot \left(\|\nabla f(x_k)\|_2^2 + \frac{\sigma^2}{n_k}\right), \tag{78a}$$

$$\nabla f(x_k)^{\mathrm{T}} \mathbb{E}_{S_k}[H_k r_k] \leq -\frac{1}{2}\beta_k \mu \|\nabla f(x_k)\|_2^2 + \beta_k^2 \cdot \mu^{-1}\left(1 + C^{-1}\right)\frac{\sigma^2}{n_k}. \tag{78b}$$

Proof. The first result (78a) is easy to obtain by considering (69a) and noticing that $1+2\alpha_k^2-2\alpha_k \leq 1$ when $\alpha_k \in [0,1]$ and $\delta_k^{-1} \leq C^{-1}\beta_k^2$. Since $\alpha_k \leq \beta_k^{\frac{1}{2}}, \delta_k \geq C\beta_k^{-2}$ and $(1+C^{-\frac{1}{2}})^2 \leq 2(1+C^{-1})$ we have

$$\begin{aligned}
\frac{1}{2}\frac{\alpha_k^2(\delta_k^{-\frac{1}{2}} + \beta_k)^2}{\beta_k \mu} \cdot \frac{\sigma^2}{n_k} &\leq \frac{1}{2}\frac{\beta_k(C^{-\frac{1}{2}}\beta_k + \beta_k)^2}{\beta_k \mu} \cdot \frac{\sigma^2}{n_k} \\
&= \frac{1}{2}\mu^{-1}(C^{-\frac{1}{2}} + 1)^2 \beta_k^2 \cdot \frac{\sigma^2}{n_k} \\
&\leq \beta_k^2 \mu^{-1}(1 + C^{-1})\frac{\sigma^2}{n_k}.
\end{aligned}$$

Substituting it into (69b), we obtain (78b). □

Using Corollary 3 we obtain the descent property of RST-AM:

Lemma 6. *Suppose that Assumptions 1 and 2 hold for $\{x_k\}$ generated by RST-AM. $C > 0$ is the constant in (12). If $0 < \beta_k \leq \frac{\mu}{4L(1+C^{-1})}, \delta_k \geq C\beta_k^{-2}, 0 \leq \alpha_k \leq \min\{1, \beta_k^{\frac{1}{2}}\}$ and satisfies (55), then*

$$\mathbb{E}_{S_k}[f(x_{k+1})] \leq f(x_k) - \frac{1}{4}\beta_k \mu \|\nabla f(x_k)\|_2^2 + \beta_k^2 \left((L + \mu^{-1})(1 + C^{-1})\right)\frac{\sigma^2}{n_k}. \tag{79}$$

Proof. According to Assumption 1, we have

$$\begin{aligned}
f(x_{k+1}) &\leq f(x_k) + \nabla f(x_k)^{\mathrm{T}}(x_{k+1} - x_k) + \frac{L}{2}\|x_{k+1} - x_k\|_2^2 \\
&= f(x_k) + \nabla f(x_k)^{\mathrm{T}} H_k r_k + \frac{L}{2}\|H_k r_k\|_2^2.
\end{aligned} \tag{80}$$

Taking expectation with respect to the mini-batch S_k on both sides of (80) and using Corollary 3 we obtain

$$\begin{aligned}
&\mathbb{E}_{S_k}[f(x_{k+1})] \\
&\leq f(x_k) + \nabla f(x_k)^{\mathrm{T}} \mathbb{E}_{S_k}[H_k r_k] + \frac{L}{2}\mathbb{E}_{S_k}\|H_k r_k\|_2^2 \\
&\leq f(x_k) - \frac{1}{2}\beta_k \mu \|\nabla f(x_k)\|_2^2 + \beta_k^2 \mu^{-1}(1 + C^{-1})\frac{\sigma^2}{n_k} + L\beta_k^2(1 + C^{-1})\left(\|\nabla f(x_k)\|_2^2 + \frac{\sigma^2}{n_k}\right) \\
&= f(x_k) - \beta_k\left(\frac{1}{2}\mu - \beta_k L(1 + C^{-1})\right)\|\nabla f(x_k)\|_2^2 + \beta_k^2(L + \mu^{-1})(1 + C^{-1})\frac{\sigma^2}{n_k}.
\end{aligned} \tag{81}$$

Then (81) combined with the assumption $\beta_k \leq \frac{\mu}{4L(1+C^{-1})}$ implies (79). □

Following the proofs in Wang et al. (2017), we introduce the definition of a *supermartingale*.

Definition 1. *Let $\{\mathcal{F}_k\}$ be an increasing sequence of σ-algebras. If $\{X_k\}$ is a stochastic process satisfying (i) $\mathbb{E}[|X_k|] < \infty$, (ii) $X_k \in \mathcal{F}_k$ for all k, and (iii) $\mathbb{E}[X_{k+1}|\mathcal{F}_k] \leq X_k$ for all k, then $\{X_k\}$ is called a supermartingale.*

Proposition 3 (Supermartingale convergence theorem, see, e.g., Theorem 4.2.12 in (Durrett, 2019))**.** *If $\{X_k\}$ is a nonnegative supermartingale, then $\lim_{k\to\infty} X_k \to X$ almost surely and $\mathbb{E}[X] \leq \mathbb{E}[X_0]$.*

Now, we prove the convergence theory of RST-AM in the nonconvex stochastic case.

Proof of Theorem 4. (i) Define $\phi_k := \frac{\beta_k \mu}{4}\|\nabla f(x_k)\|_2^2$ and $\tilde{L} := (L+\mu^{-1})(1+C^{-1})$, $\gamma_k := f(x_k) + \tilde{L}\frac{\sigma^2}{n}\sum_{i=k}^{\infty}\beta_i^2$. Let $\mathcal{F}_k$ be the σ-algebra measuring ϕ_k, γ_k, and x_k. From (79) we know that for any k,

$$\begin{aligned}\mathbb{E}[\gamma_{k+1}|\mathcal{F}_k] &= \mathbb{E}[f(x_{k+1})|\mathcal{F}_k] + \tilde{L}\frac{\sigma^2}{n}\sum_{i=k+1}^{\infty}\beta_i^2 \\ &\leq f(x_k) - \frac{1}{4}\beta_k\mu\|\nabla f(x_k)\|_2^2 + \tilde{L}\frac{\sigma^2}{n}\sum_{i=k}^{\infty}\beta_i^2 = \gamma_k - \phi_k, \end{aligned} \tag{82}$$

which implies that $\mathbb{E}[\gamma_{k+1} - f^{low}|\mathcal{F}_k] \leq \gamma_k - f^{low} - \phi_k$. Since $\phi_k \geq 0$, we have $0 \leq \mathbb{E}[\gamma_k - f^{low}] \leq \gamma_0 - f^{low} < +\infty$. As the diminishing condition (14) holds, we obtain $\mathbb{E}[f(x_k)] \leq M_f$ for some constant $M_f > 0$. According to Definition 1, $\{\gamma_k - f^{low}\}$ is a supermartingale. Therefore, Proposition 3 indicates that there exists a γ such that $\lim_{k\to\infty}\gamma_k = \gamma$ with probability 1, and $\mathbb{E}[\gamma] \leq \mathbb{E}[\gamma_0]$. Note that from (82) we have $\mathbb{E}[\phi_k] \leq \mathbb{E}[\gamma_k] - \mathbb{E}[\gamma_{k+1}]$. Thus,

$$\mathbb{E}\left[\sum_{k=0}^{\infty}\phi_k\right] \leq \sum_{k=0}^{\infty}(\mathbb{E}[\gamma_k] - \mathbb{E}[\gamma_{k+1}]) < +\infty,$$

which further yields that

$$\sum_{k=0}^{\infty}\phi_k = \frac{\mu}{4}\sum_{k=0}^{\infty}\beta_k\|\nabla f(x_k)\|_2^2 < +\infty \text{ with probability } 1. \tag{83}$$

Since $\sum_{k=0}^{\infty}\beta_k = +\infty$, it follows that (16) holds.

(ii) If the noisy gradient is bounded, i.e.,

$$\mathbb{E}_{\xi_k}[\|\nabla f_{\xi_k}(x_k)\|_2^2] \leq M_g, \tag{84}$$

where $M_g > 0$ is a constant, then a stronger result can be obtained.

For any give $\epsilon > 0$, according to (16), there exist infinitely many iterates x_k such that $\|\nabla f(x_k)\|_2 \leq \epsilon$. Then if (17) does not hold, there must exist two infinite sequences of indices $\{s_i\}$, $\{t_i\}$ with $t_i > s_i$, such that for $i = 0, 1, \ldots$, $k = s_i + 1, \ldots, t_i - 1$,

$$\|\nabla f(x_{s_i})\|_2 \geq 2\epsilon, \|\nabla f(x_{t_i})\|_2 < \epsilon, \|\nabla f(x_k)\|_2 \geq \epsilon. \tag{85}$$

Then from (83) it follows that

$$+\infty > \sum_{k=0}^{\infty}\beta_k\|\nabla f(x_k)\|_2^2 \geq \sum_{i=0}^{+\infty}\sum_{k=s_i}^{t_i-1}\beta_k\|\nabla f(x_k)\|_2^2 \geq \epsilon^2\sum_{i=0}^{+\infty}\sum_{k=s_i}^{t_i-1}\beta_k \text{ with probability } 1,$$

which implies that

$$\sum_{k=s_i}^{t_i-1}\beta_k \to 0 \text{ with probability } 1, \text{as } i \to +\infty. \tag{86}$$

According to (71) and (66), we have

$$\begin{aligned}&\mathbb{E}[\|x_{k+1} - x_k\|_2|x_k] \\ &= \mathbb{E}[\|H_k r_k\|_2|x_k] \\ &\leq \sqrt{2\left(\beta_k^2\left(1+2\alpha_k^2 - 2\alpha_k\right) + \alpha_k^2\delta_k^{-1}\right)}\mathbb{E}[\|r_k\|_2|x_k] \\ &\leq \beta_k\sqrt{2(1+C^{-1})}\mathbb{E}[\|r_k\|_2|x_k] \\ &\leq \beta_k\sqrt{2(1+C^{-1})}(\mathbb{E}[\|r_k\|_2^2|x_k])^{\frac{1}{2}} \\ &\leq \beta_k\sqrt{2(1+C^{-1})}M_g^{\frac{1}{2}}, \end{aligned} \tag{87}$$

where the last inequalities are due to *Cauchy-Schwarz inequality* and (84). Then it follows from (87) that

$$\mathbb{E}[\|x_{t_i} - x_{s_i}\|_2] \leq \sqrt{2(1+C^{-1})} M_g^{\frac{1}{2}} \sum_{k=s_i}^{t_i-1} \beta_k,$$

which together with (86) implies that $\|x_{t_i} - x_{s_i}\|_2 \to 0$ with probability 1, as $i \to +\infty$. Hence, from the Lipschitz continuity of ∇f, it follows that $\|\nabla f(x_{t_i}) - \nabla f(x_{s_i})\|_2 \to 0$ with probability 1 as $i \to +\infty$. However, this contradicts (85). Therefore, the assumption that (17) does not hold is not true. □

Proof of Theorem 5. According to (81) in Lemma 6, we have

$$\begin{aligned} &\sum_{k=0}^{N-1} \beta_k \left(\frac{1}{2}\mu - \beta_k L(1+C^{-1}) \right) \mathbb{E}\|\nabla f(x_k)\|_2^2 \\ \leq\ & f(x_0) - f^{low} + \sum_{k=0}^{N-1} \beta_k^2 (L+\mu^{-1})(1+C^{-1}) \frac{\sigma^2}{n_k}, \end{aligned} \tag{88}$$

where the expectation is taken with respect to $\{S_j\}_{j=0}^{N-1}$. Define

$$P_R(k) \stackrel{\text{def}}{=} Prob\{R=k\} = \frac{\beta_k \left(\frac{1}{2}\mu - \beta_k L(1+C^{-1})\right)}{\sum_{j=0}^{N-1} \beta_j \left(\frac{1}{2}\mu - \beta_j L(1+C^{-1})\right)},\ k=0,\ldots,N-1, \tag{89}$$

then

$$\begin{aligned} \mathbb{E}\left[\|\nabla f(x_R)\|_2^2\right] &= \frac{\sum_{k=0}^{N-1} \beta_k \left(\frac{1}{2}\mu - \beta_k L(1+C^{-1})\right) \mathbb{E}\left[\|\nabla f(x_k)\|_2^2\right]}{\sum_{j=0}^{N-1} \beta_j \left(\frac{1}{2}\mu - \beta_j L(1+C^{-1})\right)} \\ &\leq \frac{D_f + \sigma^2 (L+\mu^{-1})(1+C^{-1}) \sum_{k=0}^{N-1} \beta_k^2 / n_k}{\sum_{j=0}^{N-1} \beta_j \left(\frac{1}{2}\mu - \beta_j L(1+C^{-1})\right)}. \end{aligned} \tag{90}$$

Let $\tilde{D}$ be a problem-independent constant. If we choose $\beta_k = \beta := \min\{\frac{\mu}{4L(1+C^{-1})}, \frac{\tilde{D}}{\sigma\sqrt{N}}\}$, and $n_k = n$, then the definition of P_R simplifies to $P_R(k) = 1/N$. From (90) we have

$$\begin{aligned} \mathbb{E}[\|\nabla f(x_R)\|_2^2] &\leq \frac{D_f + \sigma^2 (L+\mu^{-1})(1+C^{-1}) \frac{N\beta^2}{n}}{\sum_{j=0}^{N-1} \beta(\frac{1}{2}\mu - \frac{\mu}{4})} \\ &= \frac{D_f + \sigma^2 (L+\mu^{-1})(1+C^{-1}) \cdot \frac{N\beta^2}{n}}{N\beta \cdot \frac{1}{4}\mu} \\ &= \frac{4D_f}{N\beta\mu} + \frac{\sigma^2 (L+\mu^{-1})(1+C^{-1}) \cdot \beta}{\frac{1}{4} n\mu} \\ &\leq \frac{4D_f}{N\mu} \max\left\{ \frac{4L(1+C^{-1})}{\mu}, \frac{\sigma\sqrt{N}}{\tilde{D}} \right\} + \frac{4\sigma^2 (L+\mu^{-1})(1+C^{-1})}{n\mu} \cdot \frac{\tilde{D}}{\sigma\sqrt{N}} \\ &\leq \frac{4D_f}{N\mu} \left(\frac{4L(1+C^{-1})}{\mu} + \frac{\sigma\sqrt{N}}{\tilde{D}} \right) + \frac{4\sigma (L+\mu^{-1})(1+C^{-1})\tilde{D}}{n\mu\sqrt{N}} \\ &= \frac{16 D_f L(1+C^{-1})}{N\mu^2} + \frac{\sigma}{\mu\sqrt{N}} \left(\frac{4D_f}{\tilde{D}} + \frac{4(L+\mu^{-1})(1+C^{-1})\tilde{D}}{n} \right). \end{aligned}$$

Therefore, to ensure $\mathbb{E}[\|\nabla f(x_R)\|_2^2] \leq \epsilon$, the number of iterations is $\mathcal{O}(1/\epsilon^2)$. □

B EXPERIMENTAL DETAILS

Our main codes were written based on the PyTorch framework [1] and one GeForce RTX 2080 Ti GPU was used for the tests in training neural networks. Our methods are ST-AM (MST-AM) and the regularized version RST-AM.

B.1 EXPERIMENTAL DETAILS ABOUT ST-AM/MST-AM

The experiments about ST-AM is conducted to verify the main theorems, i.e. Theorem 1, Corollary 1 and Theorem 2. Three types of problems are used for the experiments. The conjugate residual (CR) method is a short-term recurrence version of the full-memory GMRES and needs matrix-vector products to fulfill the algorithm. We give a pseudocode of CR method here for readers who are not familiar with this numerical algorithm.

Algorithm 4 CR Algorithm for solving a SPD linear system $Ax = b$.

Input: $x_0 \in \mathbb{R}^d$.
Output: $x \in \mathbb{R}^d$

1: $r_0 = b - Ax_0, p_0 = r_0$
2: **for** $k = 0, 1, \ldots,$ until convergence, **do**
3: $\quad \alpha_k = \frac{r_k^{\mathrm{T}} A r_k}{(Ap_k)^{\mathrm{T}} A p_k}$
4: $\quad x_{k+1} = x_k + \alpha_k p_k$
5: $\quad r_{k+1} = r_k - \alpha_k A p_k$
6: $\quad \beta_k = \frac{r_{k+1}^{\mathrm{T}} A r_{k+1}}{r_k^{\mathrm{T}} A r_k}$
7: $\quad p_{k+1} = r_{k+1} + \beta_k p_k$
8: $\quad Ap_{k+1} = Ar_{k+1} + \beta_k A p_k$
9: **end for**
10: **return** x_k

It should be pointed out that CR method needs to directly assess the matrix A, and the residual update (Line 5) is based on the linear assumption, which makes it inapplicable to nonlinear problems or the case that A is unavailable. Also, even though finite difference technique can be used to construct the matrix-vector products, the number of gradient evaluations is twice of that of ST-AM.

B.1.1 STRONGLY CONVEX QUADRATIC OPTIMIZATION

To construct a case of (5), we considered the least-squares problem:

$$\min_{x \in \mathbb{R}^d} f(x) := \frac{1}{2} \|Ax - b\|_2^2, \tag{91}$$

where $A \in \mathbb{R}^{\ell \times d}, b \in \mathbb{R}^d$, which can be reformulated as a form of (5).

We generated a dense random matrix $A \in \mathbb{R}^{500 \times 100}$ and a dense random vector $b \in \mathbb{R}^{100}$ for the test. The gradient descent used a fixed stepsize $\eta \leq \frac{1}{\|A\|_2^2}$ that can guarantee convergence, and the same η was used as the β_k for the full-memory AM and ST-AM.

We also conducted additional tests about solving the problem (91) with different condition number, where the eigenvalues of A were set to uniformly distributed. The results with different condition number ($cond(A^{\mathrm{T}}A) = 10^2, 10^4, 10^6$) are shown in Figure 4. It can be observed that the curves of CR, AM and ST-AM nearly coincide, which verify the correctness of Theorem 1. Also, since the eigenvalues are uniformly distributed, the superlinear convergence behaviour may not happen. Nonetheless, CR, AM and ST-AM are still much faster then the GD method.

B.1.2 SOLVING A NONSYMMETRIC LINEAR SYSTEM

For the solution of a nonsymmetric linear system

$$Ax = b, \tag{92}$$

[1] Information about this framework is referred tohttps://pytorch.org.

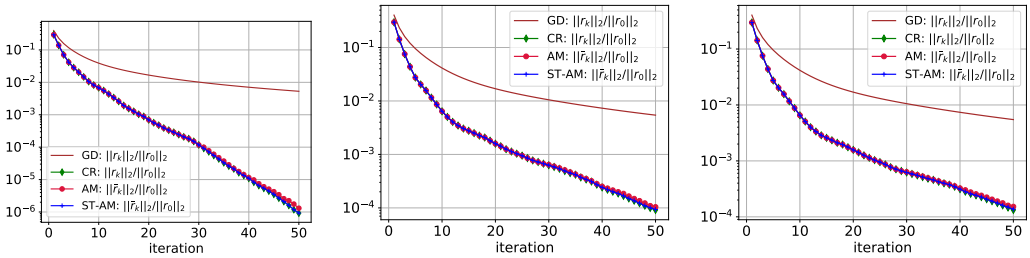

(a) $cond(A^{\mathrm{T}}A) = 1 \times 10^2$ (b) $cond(A^{\mathrm{T}}A) = 1 \times 10^4$ (c) $cond(A^{\mathrm{T}}A) = 1 \times 10^6$

Figure 4: Solving (91) with different condition number: $cond(A^{\mathrm{T}}A) = \lambda_{max}(A^{\mathrm{T}}A)/\lambda_{min}(A^{\mathrm{T}}A)$.

where $A \in \mathbb{R}^{d\times d}, b \in \mathbb{R}^d$, the fixed-point iteration (FP) is $x_{k+1} = g(x_k) := x_k + \eta(b - Ax_k)$. Theorem 2 requires g to be a contractive map, i.e. $\|I - \eta A\|_2 < 1$. We use a test matrix "fidap029" from the Matrix Market [2] This matrix is a banded matrix and not symmetric. We use Jacobi preconditioner for all the tested iterative methods. Since solving linear systems is not the main focus of this work, we did not do a thorough tests of applying ST-AM to solve various nonsymmetric linear systems.

B.1.3 Cubic-Regularized quadratic minimization

The concerned cubic-regularized quadratic minimization is

$$\min_{x\in\mathbb{R}^d} f(x) := \|Ax - b\|_2^2 + \frac{M}{3}\|x\|_2^3, \tag{93}$$

where $A \in \mathbb{R}^{\ell\times d}, b \in \mathbb{R}^d$, and $M \geq 0$ is the regularization parameter. It can be computed that

$$\nabla f(x) = A^{\mathrm{T}}(Ax - b) + M\|x\|_2 x = (A^{\mathrm{T}}A + M\|x\|_2 I)x - A^{\mathrm{T}}b.$$

Hence, for the gradient descent $x_{k+1} = g(x_k) := x_k - \eta\nabla f(x_k)$, the Jacobian of g is $(1 - M\|x\|_2)I - A^{\mathrm{T}}A$, which has $\hat{\kappa} > 0$ in the local region $\mathcal{B}(\rho)$.

We generated a dense random matrix $A \in \mathbb{R}^{500\times 100}$ and a dense vector $b \in \mathbb{R}^{100}$ for the test.

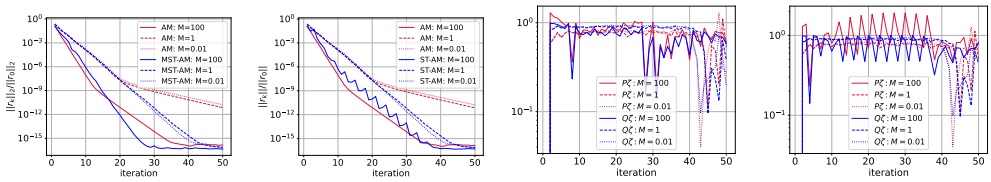

(a) MST-AM (b) ST-AM (c) MST-AM (d) ST-AM

Figure 5: Solving (93) with different M. (a) $\|r_k\|_2/\|r_0\|_2$ of MST-AM; (b) $\|r_k\|_2/\|r_0\|_2$ of ST-AM; (c) $\|P_{k-1}\zeta_k\|_2/\|\Delta x_{k-1}\|_2$ and $\|Q_{k-1}\zeta_k\|_2/\|\Delta r_{k-1}\|_2$ of MST-AM; (d) $\|P_{k-1}\zeta_k\|_2/\|\Delta x_{k-1}\|_2$ and $\|Q_{k-1}\zeta_k\|_2/\|\Delta r_{k-1}\|_2$ of ST-AM.

We also conducted the tests related to different regularization parameter M, and the cases that $M = 0.01, 1, 100$ are shown in Figure5. Figure 5 shows that with the large $M = 100$, both AM and MST-AM converge faster. An ablation study was also conducted about the boundedness restriction of $\|P_{k-1}\zeta_k\|_2, \|Q_{k-1}\zeta_k\|_2$ in Theorem 2. In Figure 5(b), we show the convergence behaviour of ST-AM without the boundedness check. In the case of the rather large regularization $M = 100$, ST-AM does not show a monotone decrease of the residual. To further investigate the cause, we plot the magnitude of $\|P_{k-1}\zeta_k\|_2/\|\Delta x_{k-1}\|_2, \|Q_{k-1}\zeta_k\|_2\|\Delta r_{k-1}\|_2$ in Figure5(c) and Figure 5(d).

[2] https://math.nist.gov/MatrixMarket/.

It can be observed that the evolutions of $\|P_{k-1}\zeta_k\|_2/\|\Delta x_{k-1}\|_2, \|Q_{k-1}\zeta_k\|_2\|\Delta r_{k-1}\|_2$ are quite oscillatory in ST-AM, while being roughly bounded below 1 in MST-AM. This phenomenon may accounts for the more stable convergence behaviour of MST-AM and verifies the necessity of the changes of MST-AM compared with ST-AM. In our experiments, we also found the restarting period can be set quite large and has little effect on ST-AM.

B.2 Experimental details about RST-AM

Our experiments on RST-AM focused on training neural networks. Since ST-AM can be regarded as a special case of RST-AM with $\delta_k^{(1)} = \delta_k^{(2)} = 0$, the basic ST-AM is also covered. In the Line 10 in Algorithm 1, α_k should be adjusted to meet the positive definiteness check (13), which can be simplified to $(\Delta x_k)^{\mathrm{T}} r_k \geq \beta_k \mu \|r_k\|_2^2$ in practice. The adjustment of α_k can be (i) $\alpha_k = \min\{\alpha_k, 2\beta_k(1-\mu)/\lambda_k\}$, or (ii) $\alpha_k = 0$. We use the option (ii) since the violation of (13) seldom happened in our tests and option (ii) is more simple to apply.

In the experiments on MNIST and Penn TreeBank, we incorporated preconditioning into the baseline method SAM and our method. Preconditioning is found to be effective for difficult problems, e.g. mini-batch training with very small batch size and the scaling of the model's parameters being important. Assuming that there is a basic optimizer $preconditioner(x_k, s_k)$, which work as a black-box procedure that updates x_k given the gradient evaluation s_k, i.e. $x_{k+1} = precondtioner(x_k, s_k)$, the preconditioned mixing of RST-AM is

$$x_{k+1} = precondtioner(\bar{x}_k, -\bar{r}_k). \tag{94}$$

which substitutes for the Line 13 in Algorithm 1. The simple mixing (Line 13 in Algorithm 1 can be seen as a special case by defining $preconditioner(x_k, s_k) = x_k - \beta_k s_k$.

B.2.1 Hyperparameter setting of RST-AM

The hyperparameters of RST-AM are easy to tune. The only hyperparameters that need carefully tuned is the regularization parameters c_1, c_2 in $\delta_k^{(1)}$ and $\delta_k^{(2)}$. We found RST-AM is more sensitive to c_1, possibly due to the fact that it influences the construction of secant equations. c_2 can be quite small in our tests. The hyperparameter C in $\delta_k^{(2)}$ was set to be very small ($C = 1 \times 10^{-16}$) so as to ensure $\delta_k^{(2)} = \frac{c_2\|r_k\|_2^2}{\|p_k\|_2^2+\epsilon_0}$ almost all the time. ϵ_0 only serves as the safe-guard to prevent the denominator from being zero. We found $\|p_k\|_2 > 0$ and $\|\Delta x_{k-1}\|_2 > 0$ always held in the tests, so ϵ_0 can be omitted. In the experiments except for deterministic optimization on MNIST, we kept the setting $c_1 = 1, c_2 = 1 \times 10^{-7}$ unchanged and found such setting is quite robust.

The other hyperparameters are α_k, β_k, which can be always initially set as 1. So RST-AM has the same number of hyperparameters to tune as SGDM, since SGDM needs to tune learning rate and the momentum.

B.2.2 Experiments on MNIST

The experiments on MNIST aimed to validate the effectiveness of RST-AM in deterministic optimization, so we only concerned about the training loss by regarding it as a nonlinear function to be optimized. The training dataset was preprocessed by randomly selecting 10k images from the total 60k images to facilitate the full-batch training.

The baselines are SGDM, Adam, Adagrad, RMSprop and SAM. We tried our best to ensure that the baselines had the best performance in the tests. We tuned the learning rates by log-scale grid-searches from 10^{-3} to 100. The learning rates of SGDM, Adam, Adagrad, RMSprop were 0.2, 0.001, 0.01, 0.001, respectively. For SAM, we used the hyperparameter setting recommended in (Wei et al., 2021).

For RST-AM, we set $c_1 = 0.05, c_2 = 1 \times 10^{-7}, \alpha_k = \beta_k = 1$. When $(\Delta x_k)^{\mathrm{T}} r_k \leq 0$ occurs, $x_{k+1} = x_k + 0.2 r_k$ was used as the new update.

For the preconditioned RST-AM, we set $c_1 = 1 \times 10^{-2}, c_2 = 1 \times 10^{-7}$ for the Adagrad-preconditioned RST-AM and $c_1 = 1 \times 10^{-2}, c_2 = 1 \times 10^{-8}$ for the RMSprop-preconditioned RST-AM.

For all these tests, the model was trained for 200 epochs.

B.2.3 EXPERIMENTS ON CIFAR

For this group of experiments, we followed the same setting of training ResNet in (He et al., 2016). The batchsize is set to be 128 as commonly suggested. When training for N iterations, the learning rate was decayed at the $(\lfloor \frac{N}{2} \rfloor)$-th and the $(\lfloor \frac{3}{4}N \rfloor)$-th iterations. For SAM and RST-AM, the learning rate decay means decaying α_k, β_k simultaneously. The experiments were run with 3 random seeds.

The baseline optimizers were SGDM, Adam, AdaBound (Luo et al., 2019), AdaBelief (Zhuang et al., 2020), Lookahead (Zhang et al., 2019) and AdaHessian (Yao et al., 2021). AdaBound and AdaBelief are recently proposed adaptive learning rate methods to improve Adam. Lookahead is a k-step method, which can be seen as a simple sequence interpolation method. In each cycle, Lookahead iterates with an inner-optimizer $optim$ for k steps and then interpolates the first and the last iterates to give the starting point of the next cycle. Compared to Adam, AdaHessian uses Hessian-vector products to construct a diagonal approximation of the Hessian.

Since tuning hyperparameter in large model is very time-consuming, the hypermeters of each optimizers were tuned through experiments on CIFAR-10/ResNet20. For each optimizer, the hyperparameter setting that has the best final test accuracy on CIFAR-10/ResNet20 was kept unchanged and used for the other tests. We list the hyperparameters of all the tested optimizers here. (Learning rate is abbreviated as lr.)

- **SGDM**: lr = 0.1, momentum = 0.9, weight-decay = 5×10^{-4}, lr-decay = 0.1.
- **Adam**: lr = 0.001, $(\beta_1, \beta_2) = (0.9, 0.999)$, weight-decay = 5×10^{-4}, lr-decay = 0.1.
- **AdaBound**: lr = 0.001, $(\beta_1, \beta_2) = (0.9, 0.999)$, final_lr: 0.1, gamma: 0.001, weight-decay: 5×10^{-4}.
- **AdaBelief**: lr = 0.001, $(\beta_1, \beta_2) = (0.9, 0.999)$, eps = 1×10^{-8}, weight-decay = 5×10^{-4}, lr-decay = 0.1.
- **Lookahead**: $optim$: SGDM (lr = 0.1, momentum = 0.9, weight-decay = 1×10^{-3}), $\alpha = 0.8$, steps = 10, lr-decay = 0.1.
- **AdaHessian**: lr = 0.15, $(\beta_1, \beta_2) = (0.9, 0.999)$, eps=$1 \times 10^{-4}$, hessian-power: 1, weight-decay: $5 \times 10^{-4}/0.15$, lr-decay: 0.1.
- **SAM(2)**: $optim$: SGDM (lr = 0.1, momentum = 0, weight-decay = 1.5×10^{-3}), $\alpha_k = 1.0, \beta_k = 1.0, c_1 = 0.01, p = 1, m = 2$, weight-decay = 1.5×10^{-3}, lr-decay = 0.06.
- **SAM(10)**: $optim$: SGDM (lr = 0.1, momentum = 0, weight-decay = 1.5×10^{-3}), $\alpha_k = 1.0, \beta_k = 1.0, c_1 = 0.01, p = 1, m = 10$, weight-decay = 1.5×10^{-3}, lr-decay = 0.06.
- **RST-AM**: $c_1 = 1, c_2 = 1 \times 10^{-7}, \alpha_0 = \beta_0 = 1$, weight-decay = 1×10^{-3}, lr-decay = 0.1.

For the tests of SGDM, Adam, AdaBelief, Lookahead and SAM(10), we found consistent numerical results as those in (Wei et al., 2021), so we reported their results of these methods in the main paper.

Figure 6 shows the test accuracy of different optimizers for training ResNet18/WRN16-4 on CIFAR-10 and ResNeXt50/DenseNet121 on CIFAR-100. The full results of final test accuracy are listed in Table 1 in the main paper. From Figure 6, we find that the convergence behaviour of RST-AM is less erratic than SAM(10) and SAM(2). In the first 80 epochs, RST-AM converges faster than SAM, partly due to using a smaller weight decay. The learning rate schedule has a large impact on the convergence of each optimizer. Similar to SAM(10), RST-AM can always climb up and stabilize to a higher test accuracy in the final 40 epochs. It is found that RST-AM is comparable to SAM(10), while improving the short-memory SAM(2).

Since our hyperparameter tuning was conducted on CIFAR10/ResNet20, we give some results about the hyperparameters on this model.

Effect of c_2 in RST-AM. Figure 7 shows the effect of c_2, where we kept $c_1 = 1$, weight-decay=5×10^{-4} fixed, and $c_2 = 10^{-1}, 10^{-3}, 10^{-5}, 10^{-7}, 10^{-9}$. It indicates that RST-AM is not sensitive to c_2.

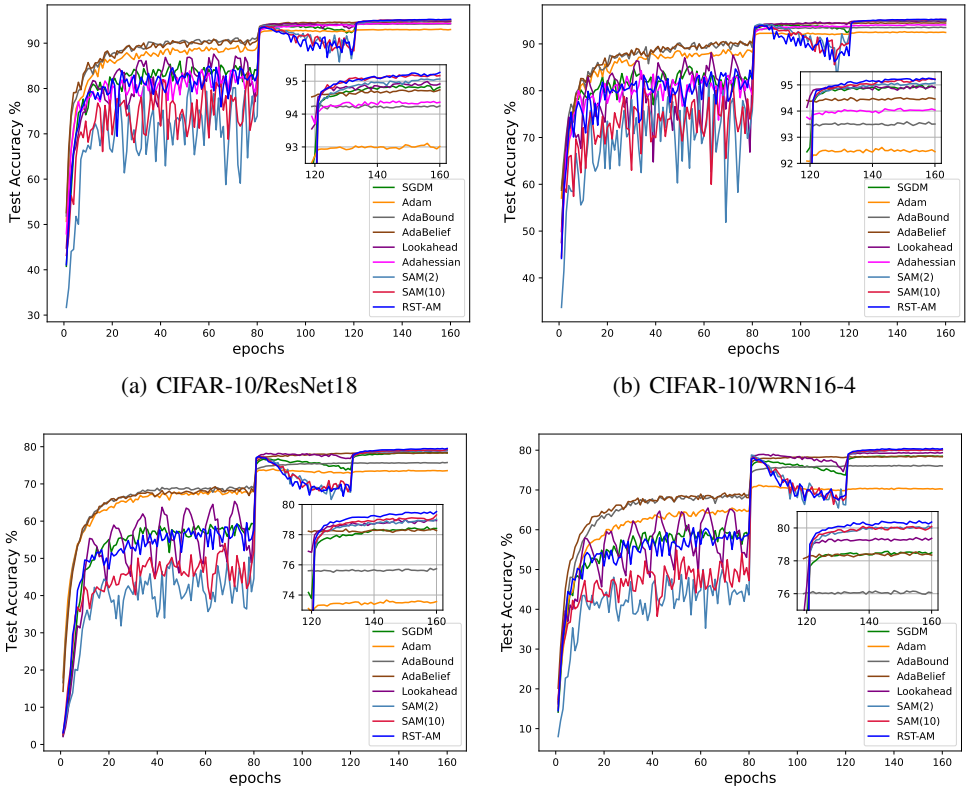

(a) CIFAR-10/ResNet18

(b) CIFAR-10/WRN16-4

(c) CIFAR-100/ResNeXt50

(d) CIFAR-100/DenseNet121

Figure 6: Test accuracy of ResNet18/WideResNet16-4 on CIFAR-10 and ResNeXt50/DenseNet121 on CIFAR-100.

Effect of c_1 in RST-AM. Figure 8 shows the effect of c_1, where we kept $c_2 = 10^{-7}$, weight-decay=5×10^{-4} fixed, and $c_1 = 0.01, 0.1, 1, 10$. It suggests that with smaller c_1, RST-AM converges faster in terms of train accuracy, but the test accuracy is worse.

Effect of weight decay in RST-AM. Weight-decay is a common hyperparameter that can affect the generalization of each optimizer. In Figure 9, we show the convergence behaviour of RST-AM with different weight-decays. It suggests that with small weight-decay, RST-AM tends to be overfitting in the test dataset.

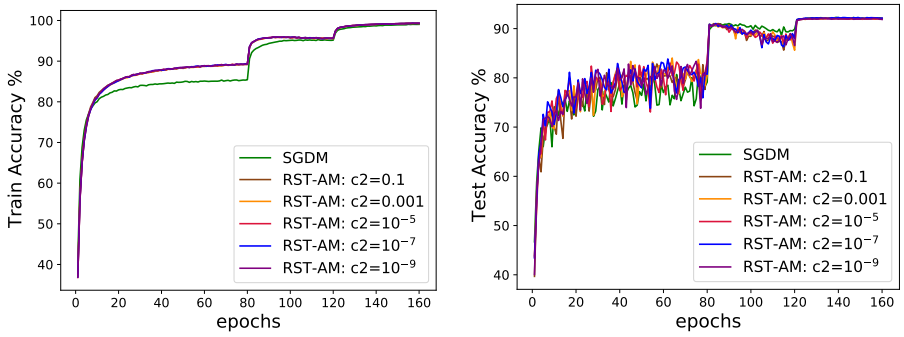

(a) Train accuracy

(b) Test accuracy

Figure 7: Train accuracy and test accuracy of RST-AM with different c_2.

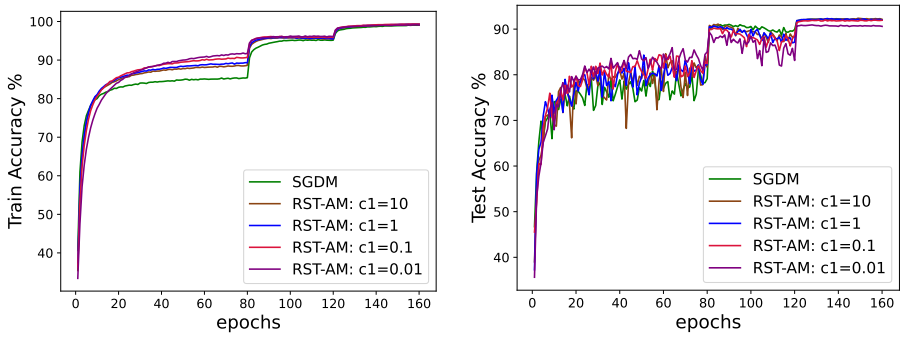

(a) Train accuracy (b) Test accuracy

Figure 8: Train accuracy and test accuracy of RST-AM with different c_1.

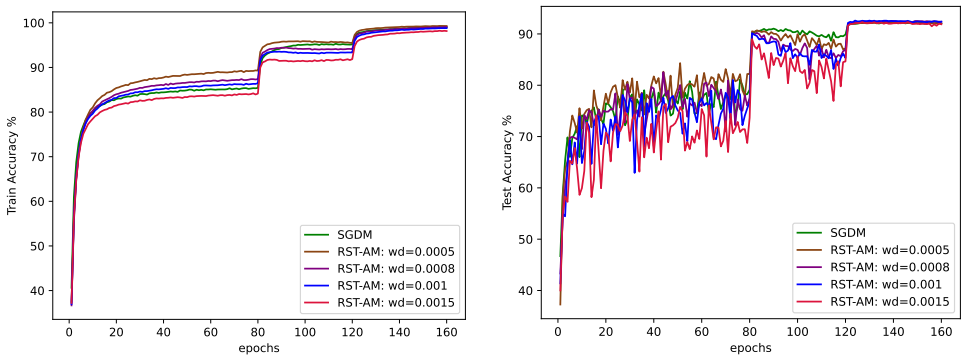

(a) Train accuracy (b) Test accuracy

Figure 9: Train accuracy and test accuracy of RST-AM with different weight-decays.

Table 5: The cost and final test accuracy compared with SGD. Memory, per-epoch time, total training epochs, total running time, and accuracy are abbreviated as "m","t/e", "e", "t", "a", respectively.

Cost (× SGDM) & accuracy	CIFAR10/ResNet18 m	t/e	e	t	a(%)	CIFAR10/WRN16-4 m	t/e	e	t	a(%)
SGDM	1.00	1.00	1.00	1.00	94.82	1.00	1.00	1.00	1.00	94.90
SAM(10)	1.73	1.78	0.56	1.00	94.81	1.26	1.28	0.63	0.80	94.94
RST-AM	1.05	1.46	0.56	0.82	94.84	1.03	1.14	0.63	0.71	94.95
Cost (× SGD) & accuracy	**CIFAR100/ResNeXt50 m**	**t/e**	**e**	**t**	**a(%)**	**CIFAR100/DenseNet121 m**	**t/e**	**e**	**t**	**a(%)**
SGDM	1.00	1.00	1.00	1.00	78.41	1.00	1.00	1.00	1.00	78.49
SAM(10)	1.30	1.16	0.50	0.58	78.37	1.16	1.19	0.50	0.60	78.84
RST-AM	1.04	1.07	0.50	0.54	78.39	1.01	1.11	0.50	0.55	78.90

Table 1 in the main paper reports the test accuracy of each optimizer when training for the same epochs. In fact, as shown in Figure 10, within 100 epochs, RST-AM can achieve a better test accuracy than SGD. So if the running time of the training process matters, it is expected that RST-AM can use less total running time due to the large number of reduction in training epochs. In Table 2, we set SGD as the baseline, and compare the computation and memory cost with SGD.

In Table 5, we give more details about the saving in training epochs and the final test accuracy. It can be seen that RST-AM can achieve comparable or better test accuracy than SGDM with less computation time, while reducing the memory footprint of SAM.

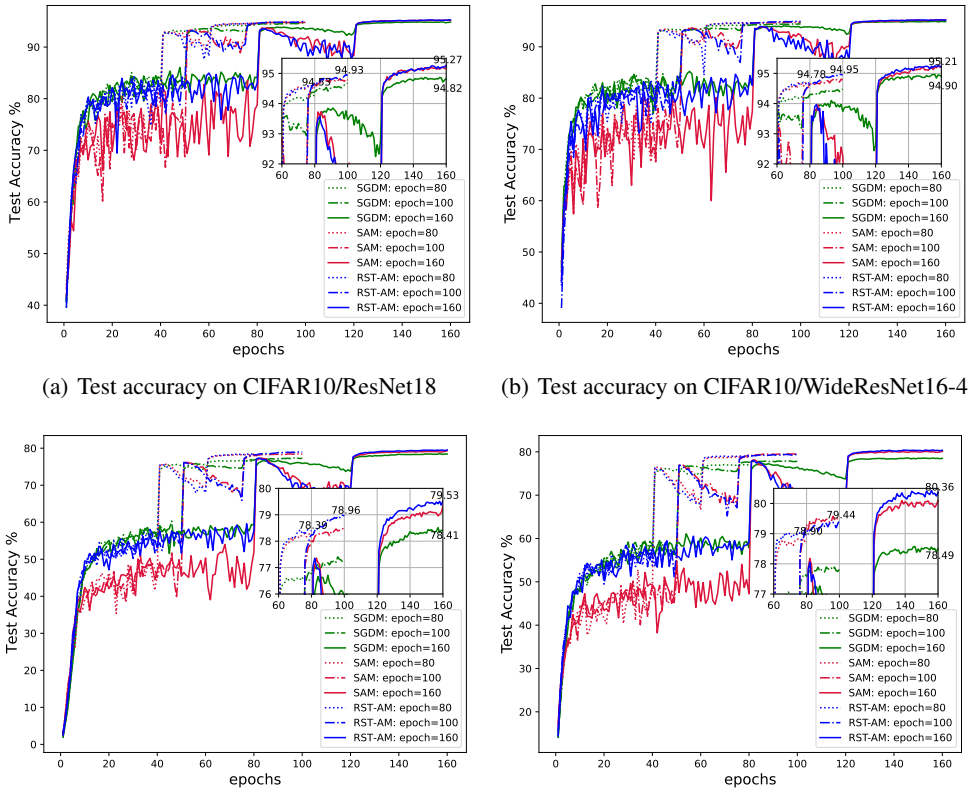

(a) Test accuracy on CIFAR10/ResNet18

(b) Test accuracy on CIFAR10/WideResNet16-4

(c) Test accuracy on CIFAR100/ResNeXt50

(d) Test accuracy on CIFAR100/DenseNet121

Figure 10: Training deep neural networks for 80,100,160 epochs. We report the final test accuracy of RST-AM for training 80,100,160 epochs at nearby point in the nested figure. The final test accuracy of SGDM for training 160 epochs is also reported for comparison.

B.2.4 Experiments on Penn TreeBank

Our experimental setting on training LSTM models on Penn TreeBank dataset is based on the official implementation of AdaBelief (Zhuang et al., 2020). Results in Table 3 were measured across 3 repeated runs with independent initialization. The parameter setting of the LSTM models are the same as that of AdaBelief. The baseline optimizers are SGDM, Adam, AdaBelief, Lookahead and SAM. We tuned hyperparameters on the validation dataset for each optimizer.

For SGDM, we tuned the learning rate (abbr. lr) via grid-search in $\{1, 10, 30, 100\}$ and found that lr=10 performs best on 2,3-layer LSTM. For 1-layer LSTM, we set lr=30 and momentum=0 as that in AdaBelief because we found such setting is better.

For Adam, we tuned the learning rate via grid-search in $\{1\times10^{-3}, 2\times10^{-3}, 5\times10^{-3}, 8\times10^{-3}, 1\times10^{-2}, 2\times10^{-2}\}$ and found 5×10^{-3} performs best.

For AdaBelief, we tuned the learning rate and found 5×10^{-3} is better than 1×10^{-2} used in (Zhuang et al., 2020).

For SAM, we used the recommended setting in (Wei et al., 2021) and used the baseline Adam as the preconditioner for SAM. Historical lengths of $m = 2$ and $m = 10$ were tested for SAM, i.e. denoted as SAM(2), SAM(10), respectively.

For our method RST-AM, we kept $c_1 = 1, c_2 = 1 \times 10^{-7}$ unchanged and used the same precondtioner (Adam) as SAM.

The batch size is 20. We trained for 500 epochs and decayed the learning rate by 0.1 at the 250th and 375th epoch.

In Table 6, we report the memory footprint and per-epoch running time of SAM(10) and RST-AM compared with Adam. It indicates that RST-AM also largely reduces the memory overhead of the long-memory SAM(10) in the language model task. Since the batch size is very small, the cost of stochastic gradient evaluation is quite cheap, which makes the additional cost of matrix computation in RST-AM and SAM(10) become considerable. However, if we consider achieving a comparable validation/test perplexity as that of Adam, RST-AM does not need to train for the same number of epochs as Adam. Table 7 shows the test perplexity of Adam, SAM(2), SAM(10), and RST-AM for training 200 epochs. By comparing the results of Table 3 and Table 7, we see RST-AM is better than Adam with much less training epochs, thus RST-AM can save a large amount of training time, as shown in Table 6.

Table 6: The cost to achieve comparable results of Adam. Memory, per-epoch time and total running time are abbreviated as "m","t/e" and "t", respectively.

Cost	1-Layer			2-Layer			3-Layer		
($\times$ Adam)	m	t/e	t	m	t/e	t	m	t/e	t
Adam	1.00	1.00	1.00	1.00	1.00	1.00	1.00	1.00	1.00
SAM(10)	1.20	1.84	0.74	1.36	1.88	0.75	1.90	1.67	0.67
RST-AM	1.06	1.73	0.69	1.15	1.78	0.71	1.11	1.53	0.61

Table 7: Test perplexity on Penn TreeBank for 1,2,3-layer LSTM (200 epochs). Lower is better.

Method	1-Layer	2-Layer	3-Layer
Adam	80.88±.15	64.54±.18	60.34±.22
SAM(2)	81.82±.09	66.62±.26	61.55±.11
SAM(10)	**79.30±.12**	**63.21±.02**	59.47±.07
RST-AM	79.49±.11	63.61±.26	**59.34±.23**

B.2.5 Experiments on adversarial training

The adversarial training considers the *empirical adversarial risk minimization* (EARM) problem:

$$\min_{x \in \mathbb{R}^d} \frac{1}{T} \sum_{i=1}^{T} \max_{\|\bar{\xi}_i - \xi_i\|_2 \leq \epsilon} f_{\bar{\xi}_i}(x), \tag{95}$$

where $\bar{\xi}_i$ is the i-th adversarial data within the ϵ-ball centered at ξ_i. We followed the standard PGD adversarial training in (Madry et al., 2018), using projection gradient descent (PGD) to solve the inner maximization problem and the tested optimizers (SGD and RST-AM) to solve the outer minimization problem. The experiments were conducted on CIFAR10/ResNet18, CIFAR10/WRN16-4, CIFAR100/ResNet18, and CIFAR100/DenseNet121. We trained the neural networks for 200 epochs and decayed the learning rate at the 100th and 150th epoch.

Since adversarial training is much more time consuming than the ordinary training in Section B.2.3, we tuned the hyperparameters in CIFAR10/ResNet20, and applied the same hyperparameters to other models. We found the setting that $c_1 = 1, c_2 = 1 \times 10^{-7}$ and weight-decay = 0.001 is still suitable for this task.

The CIFAR-10 (CIFAR-100) dataset contains 50K images for training and 10K images for testing. Since it is found that the phenomenon of overfitting is severer (Rice et al., 2020) in adversarial training, we randomly selected 5K images from the total 50K training dataset as the validation dataset (the other 45K images remained as the training dataset), and chose the best checkpoint model in the validation set to evaluate on the test dataset. We consider two types of test accuracy:
(i) the clean test accuracy, where clean data was used for model evaluation;
(ii) the robust test accuracy, where corrupted data was used for model evaluation. The attacking methods are FGSM (Goodfellow et al., 2014), PGD-20 (Madry et al., 2018), and C&W$_\infty$ attack (Carlini & Wagner, 2017).

Table 8: Test accuracy (%) for adversarial training.

Optimizer	CIFAR10/ResNet18				CIFAR100/DenseNet121			
	Clean	FGSM	PGD-20	C&W$_\infty$	Clean	FGSM	PGD-20	C&W$_\infty$
SGD	82.16	63.23	51.91	50.22	59.45	39.76	30.92	29.00
RST-AM	82.53	63.78	52.43	50.52	60.48	40.41	31.20	29.52
Optimizer	**CIFAR10/WRN16-4**				**CIFAR100/ResNet18**			
	Clean	FGSM	PGD-20	C&W$_\infty$	Clean	FGSM	PGD-20	C&W$_\infty$
SGD	80.84	60.97	49.29	47.62	55.42	36.17	28.18	26.31
RST-AM	81.36	61.38	49.93	47.95	56.49	37.00	28.50	26.66

In Tabel 8, we report the average results of tests with three different random seeds. It can be found that RST-AM can achieve both higher clean test accuracy and robust test accuracy across various models on CIFAR10/CIFAR100. To see the convergence behaviour of SGD and RST-AM, we plot the curves of the clean validation accuracy and the PGD-10 attacked validation accuracy in Figure 11. We can observe the phenomenon of robust overfitting (Rice et al., 2020) from these curves, which justifies our experimental setting with validation set for the checkpoint selection. Nonetheless, the numerical results suggests that RST-AM can still be better than SGDM in adversarial training.

It is also found that due to the heavy cost of gradient evaluations in PGD adversarial training, the additional computational cost incurred by RST-AM is negligible and the per-epoch running time of SGD and RST-AM is roughly the same. So we do not report it here.

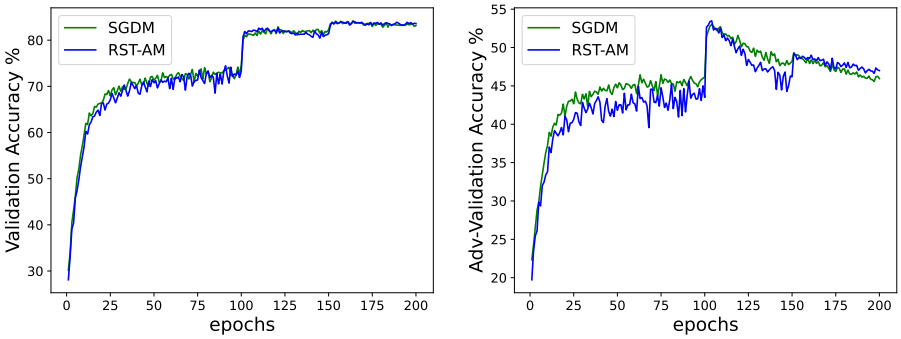

(a) CIFAR10/ResNet18

(b) CIFAR10/ResNet18

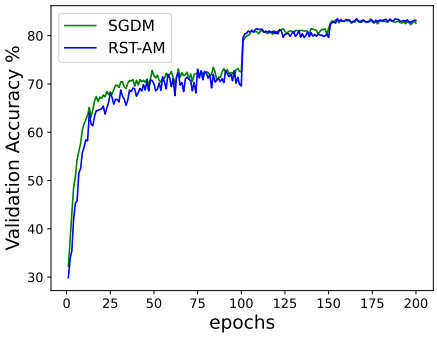

(c) CIFAR10/WRN16-4

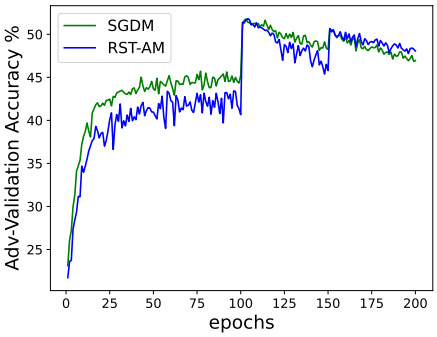

(d) CIFAR10/WRN16-4

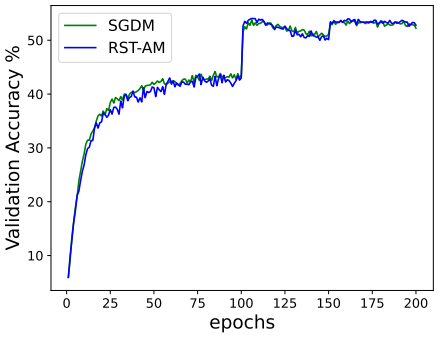

(e) CIFAR100/ResNet18

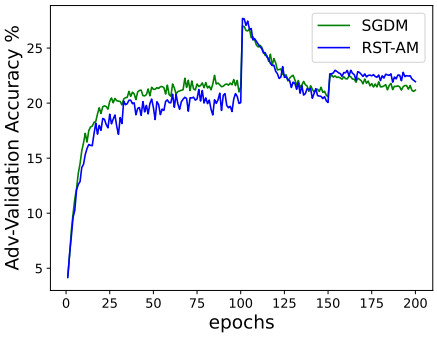

(f) CIFAR100/ResNet18

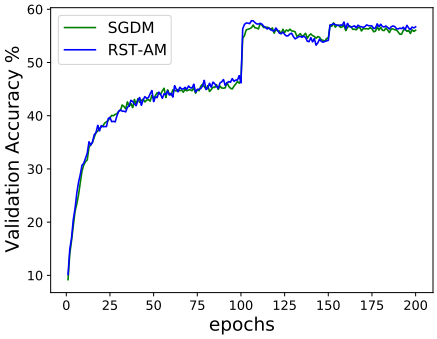

(g) CIFAR100/DenseNet121

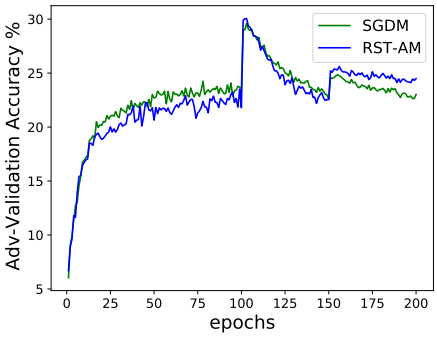

(h) CIFAR100/DenseNet121

Figure 11: Clean accuracy and PGD-10 attacked accuracy on the validation set in training different neural networks.